

1 *Accepted version of Review Article for Royal Society Interface Focus issue on: 'The origin and rise of*
2 *complex life: integrating models, geochemical and paleontological data'*

3 On the use of models in understanding 4 the rise of complex life

5 **Timothy M. Lenton**

6 Global Systems Institute, University of Exeter, Exeter EX4 4QE, UK (t.m.lenton@exeter.ac.uk)

7 Abstract

8 Recently several seemingly irreconcilably different models have been proposed for relationships
9 between Earth system processes and the rise of complex life. These models provide very different
10 scenarios of Proterozoic atmospheric oxygen and ocean nutrient levels, whether they constrained
11 complex life, and of how the rise of complex life affected biogeochemical conditions. For non-
12 modellers it can be hard to evaluate which – if any – of the models and their results have more
13 credence – hence this article. I briefly review relevant hypotheses, how models are being used to
14 incarnate and sometimes test those hypotheses, and key principles of biogeochemical cycling
15 models should embody. Then I critically review the use of biogeochemical models in: inferring key
16 variables from proxies; reconstructing ancient biogeochemical cycling; and examining how complex
17 life affected biogeochemical cycling. Problems are found in published model results purporting to
18 demonstrate long-term stable states of very low Proterozoic atmospheric pO_2 and ocean P levels. I
19 explain what they stem from and highlight key empirical uncertainties that need to be resolved.
20 Then I suggest how models and data can be better combined to advance our scientific understanding
21 of the relationship between Earth system processes and the rise of complex life.

22 Keywords

23 Earth system; biogeochemical cycling; complex life; modelling; oxygen; phosphorus

24 Introduction

25 As complex and self-aware organisms, some of us are fascinated by the origin and rise of complex
26 life – because it is a key part of our origins. As well as establishing when those origins were, and in
27 what order things evolved, as scientists we are drawn to questions of causality: Were those origins
28 determined by intrinsic controls on biological evolution, by abiotic factors, or by a more complex
29 interplay between living and non-living parts of the Earth system? How did the rise of complex life in
30 turn alter the Earth system? And how can we gain knowledge about any causal relationships, given
31 the hundreds of millions of years that have passed since?

32 At the Discussion meeting behind this Special Issue, Jochen Brocks asked: What is the role of models
33 in understanding the rise of complex life? And how should non-modellers view their results? This
34 review is an attempt to answer those queries. For non-modellers, models can be ‘black boxes’
35 playing an opaque role in gaining scientific knowledge. This can insulate models and modellers from
36 critical scrutiny. Hence this paper aims to expose and explore the ways in which models are being
37 used to address the relationships between biogeochemical processes and the rise of complex life.

38 The broad time correlation between the rise of complex life and huge changes in the Earth system –
39 including the carbon cycle and climate – during the Neoproterozoic Era, has led many researchers to
40 assume there is a causal connection between them. However, there are currently very different
41 perspectives on the direction(s) of causality. One perspective argues that environmental constraints
42 held back the evolution [1] – or rise to ecological prominence [2] – of complex life. An opposing
43 perspective argues that complex life evolved and then it altered ecological and environmental
44 conditions [3]. A co-evolutionary feedback perspective combines elements of these two positions,
45 arguing that complex life transformed ecology and biogeochemical cycling, feeding back into its

46 subsequent evolution [4]. Other important perspectives recognise the challenging evolutionary-
47 developmental aspects of animal origins [5], and consider how unusual environmental conditions
48 may have triggered (rather than suppressed) their origin [6].

49 Modelling has been used to varying degrees to represent and sometimes to test different
50 hypotheses for the relationship between complex life and Earth system processes. Predominantly
51 this has been biogeochemical modelling. Modelling of the ecological changes associated with the
52 rise of complex life is less common. Modelling the physiology of early complex life is even rarer, and
53 modelling the evolutionary dynamics of the rise of complex life has only been attempted in the
54 generic spirit of evolutionary theory. Hence this review focuses predominantly on biogeochemical
55 modelling – but the forward look considers other approaches.

56 First, I briefly review relevant hypotheses concerning the relationships between the rise of complex
57 life and Earth system processes, the different roles that models can play in understanding deep time,
58 and the key biogeochemical principles models should embody. Then I critically review published
59 model approaches to inferring key environmental conditions from proxies; understanding
60 Proterozoic biogeochemical cycling; and modelling how complex life altered biogeochemical
61 conditions. I consider what all the current biogeochemical models may be missing. Then I suggest
62 ways forward for modelling to help improve our understanding of the rise of complex life.

63 Relevant hypotheses

64 Complex life means more here than just animals (Metazoa). Currently there is much interest in
65 whether the late rise of algae to ecological prominence, detected in the biomarker record in the
66 Cryogenian Period, was due to chronically limiting nutrient levels beforehand [7]. More prominently,
67 it has long been argued [8] that a lack of oxygen held back the evolution – or at least the radiation –
68 of animal life. Recently it became apparent that oxygen levels would have to have been very low to
69 have constrained the evolution or ecological expansion of sponges (the basal animals) [9] and

70 several other (subsequently evolved) types of animal life [2]. One response to this has been to argue
71 that Proterozoic atmospheric oxygen levels were in fact much lower than previously thought [1].
72 Another response has been to argue that oxygen constrained particular eco-physiological traits of
73 animal life, if not its origin [10]. Yet another response has been to reject the role of oxygen as a
74 constraint altogether [3]. Other candidate environmental constraints have occasionally been
75 considered, for example, too much toxic hydrogen sulphide suppressing eukaryotes [11].

76 A different view is that the evolution of complex life was just intrinsically difficult and slow and its
77 timing had nothing to do with environmental conditions or constraints. However, given natural
78 selection occurs, and given evidence of changes in environmental variables known to affect the
79 physiology and ecology of animals, it seems odd to rule out some role for the environment in the
80 evolution of complex life – even if the pertinent ‘environment’ is a localised and ecological context
81 selecting some traits over others. Furthermore, highly differentiated animals with apoptosis
82 (programmed cell death) pose their own evolutionary puzzle, as they represent a major evolutionary
83 transition to a new level of selection [12]. Explaining such transitions remains a major subject of
84 evolutionary enquiry. It generally needs special conditions in which between-group variation and
85 selection outweighs within-group variation and selection [13]. One hypothesis is that extreme
86 environmental conditions – in particular the ‘snowball Earth’ events – could have altered the
87 selective environment in a way that favoured animal evolution [6].

88 Once they had evolved, complex life forms could affect ecology and biogeochemical cycling [3, 4, 14-
89 16]. Several hypotheses have been proposed: By grazing on the smallest (cyanobacterial)
90 phytoplankton cells, the first predatory protists (using phagocytosis) could have created a niche for
91 larger (algal) phytoplankton cells, which in turn created a niche for larger predators, and so on – thus
92 starting to create a size-structured community [16]. The advent of larger phytoplankton cells could
93 have increased the efficiency of the biological pump (sinking of organic matter through the water
94 column) [4]. The evolution of filter-feeding sponges, which filter out the smallest phytoplankton

95 cells, could also have selected for larger (eukaryotic) algae and strengthened the biological pump [4].
96 When planktonic animals with through-guts and faecal pellets evolved this could have further added
97 to the efficiency of the biological pump [14]. Sessile benthic animals including sponges and
98 'rangeomorph' fronds could have concentrated resources where they were located on the
99 sediments [17]. When mobile, burrowing, bioturbating animals evolved they could have oxygenated
100 the upper sediments altering the cycling of phosphorus, carbon and sulphur and ultimately the
101 oxygen content of the atmosphere [18, 19].

102 Uses of models

103 Models are currently being used in several ways to probe potential causal relationships between
104 Earth system processes and the rise of complex life. Biogeochemical models, in particular, are being
105 used: to interpret proxy data; to explore how the ancient world could have worked; and to try to
106 establish how it did work by testing hypotheses against data. There are two principal scientific
107 targets for this modelling: to establish Proterozoic biogeochemical conditions; and to quantify the
108 potential effects of complex life on those conditions.

109 General considerations

110 A model should be as simple as possible but not too simple, following Einstein's advice. Hence users
111 of model results should always look critically at whether the underlying model is too simple or
112 unnecessarily complex to address the question at hand. All models must obey some basic principles
113 of consistency with well-established constraints – such as conservation of matter. In our focal
114 context, a model may need to capture some of the spatial heterogeneity of biogeochemical
115 conditions – but no more than necessary to accurately capture key process controls. Models should
116 also be grounded in sound process representations, ideally ones that have empirical support, which
117 in this context, usually means from studies of contemporary or more recent Earth system processes.
118 If a model contains ad hoc process representations, or representations that are clearly at odds with
119 current scientific understanding, then its results should be questioned. We should ask how those

120 results are sensitive to changing the process representations that we have doubts about. (This
121 means performing a ‘structural’ sensitivity analysis where functional forms are varied, not just a
122 more typical parameter sensitivity analysis where only parameter values are varied.) If the modellers
123 do not provide an answer we should suspend judgement on whether their model is telling us
124 anything meaningful or useful about the ancient world.

125 [Inferring key variables from proxies](#)

126 In almost all deep time cases, a model is necessary to convert a proxy measurement into an Earth
127 system property (environmental parameter) of interest. For hypotheses surrounding the rise of
128 complex life, key Earth system properties that we would like to know include: the oxygen content of
129 the atmosphere, the redox state of the ocean, the levels of limiting nutrients in the ocean, and the
130 productivity of the biosphere. Sometimes the role of models in proxy interpretation is well hidden –
131 the presence of a model may not be mentioned at all – but there is always some model involved
132 (however simple) whenever we are dealing with a ‘proxy’ – i.e. we do not have a direct
133 measurement of our variable of interest. Sometimes the absence of some proxy is used, via a model,
134 to infer a constraint on a variable of interest – adding the familiar complication that “absence of
135 evidence is not evidence of absence”.

136 [Exploring how the world could have worked](#)

137 Models are also used, more ambitiously, to help us think in a qualitatively and quantitatively
138 consistent way about how the world *could* work – in this case how the Earth system and its
139 relationship with complex life could work. The ‘Earth system’ modelling challenge here is generally
140 greater than the interpretation of proxy data, because it demands making an internally-consistent
141 model of the whole world, or at least pertinent aspects of it. The exercise can be insightful, in
142 particular in limiting what may otherwise seem like a very large ‘possibility space’, because the act of
143 building an internally-consistent model usually significantly limits the range of behaviours and results
144 it can exhibit. Making the model obey well-established constraints – such as closure of

145 biogeochemical cycles and conservation of Earth's surface redox balance – can be critical in this (and
146 in the next section I outline some of these key principles). Nevertheless, exploring how the ancient
147 world *could* have worked is not the same as establishing how it *did* work.

148 Testing hypotheses to establish how the world did work

149 To help to establish how the ancient world actually *did* work, we need to be able to test and falsify
150 hypotheses for causal relationships. That means we need to use data from the time(s) in question to
151 test our models against. Thus we need to combine models of how the Earth could have worked with
152 proxy data. This means modelling the link between variables of interest and available proxies, as well
153 as modelling the controls on the variables of interest. Here the role of the model is to incarnate
154 (represent) mechanistic hypotheses, and make quantitative predictions from those hypotheses of
155 variables that are detectable in the geologic record. That 'testbed' data needs to be independent
156 from any data that is used to drive the model (to avoid circular reasoning), and for the comparison of
157 model with data to be possible, the model has to predict observable proxy variable(s). There are
158 numerous caveats here, not least that there are always a multitude of wrong models that can
159 successfully fit any given data. However, if the model cannot fit the data it pertains to predict, and
160 we think the data are reliable, then clearly there is something wrong with the model and it can be
161 said to be *falsified* (at least in some part). Increasing the number of independent data targets we try
162 to get the model to predict generally increases the chances of falsifying the model (lowers the
163 success rate). However, here we must be wary of modellers making a model more complex as that
164 just increases the potential field of successful but wrong models.

165 Key principles of biogeochemical cycling

166 To help readers evaluate models of Proterozoic conditions, and the potential effects of complex life
167 on those conditions, it is important to review some basic principles of biogeochemical cycling.

168 Timescale separation and material balances

169 Different key Earth system variables have different natural timescales (Figure 1), and those
170 timescales are separated in a way that can help us to understand Earth system functioning and
171 simplify our modelling. For material variables like the oxygen content of the atmosphere-ocean or
172 the phosphorus content of the ocean it is standard to define a mean residence time for an atom or
173 molecule in the reservoir – that is the size of the reservoir divided by its input/output flux [20].
174 Response timescales in the presence of feedback can also be defined [20]. Over timescales
175 comparable to or longer than the residence time, the inputs to and outputs from the reservoir must
176 be in close balance, otherwise the constituent would build up indefinitely or disappear [20]. The
177 timescale(s) we are interested in determine what processes we need to include in our models.
178 Things that change much slower than our timescale(s) of interest can be treated as approximately
179 constant (and excluded from our model). Things that change much faster than our timescale(s) of
180 interest can be assumed to be close to ‘steady state’ – i.e. with inputs and outputs in balance (which
181 does not mean they are constant). However, we must consider the processes setting that steady
182 state and whether and how they (and the resulting steady state) change with the slower variables.

183 The origin and rise of complex life played out over hundreds of millions of years, after a preceding
184 Proterozoic state that persisted for a billion years. Over these timescales, there could have been
185 significant material exchanges between the crust and the mantle [21], which most models neglect,
186 as well as ~500 Myr supercontinent (Wilson) cycles. Crucially, models must include the exchange of
187 matter (including electrons/redox equivalents) with sedimentary rock reservoirs that are recycled by
188 plate tectonics over ~100 Myr timescales. As Bob Garrels and colleagues first showed in the 1970s,
189 enforcing the conservation of key elements and electrons across sedimentary reservoirs and the
190 ocean-atmosphere system provides a powerful constraint on models, enabling reconstruction of key
191 variables such as CO₂ and O₂ consistent with major (C, S) isotope records [22-24].

192 The surface, fluid aspects of the Earth system – the oceans and atmosphere (including the
193 biosphere) and different reservoirs of matter within them – generally have shorter timescales than
194 sedimentary rocks. Today, sulphate in the ocean has a residence time of ~12 million years, oxygen in
195 the atmosphere(-ocean-biosphere) ~6 million years (with respect to exchange with the crust),
196 carbon dioxide and dissolved inorganic carbon (DIC) in the ocean-atmosphere ~500,000 years,
197 phosphorus in the ocean ~20,000 years, and nitrogen in the ocean ~5,000 years. The timescale
198 separation between variables means, for example, that today we can consider oxygen to be
199 approximately constant over the timescales over which phosphorus varies, or conversely when
200 considering timescales of variation in atmospheric oxygen, phosphorus must be close to steady
201 state. However, in the Proterozoic we should consider whether residence times were quite different,
202 including whether some constituents had a shorter timescale than the ~1,000 year ocean mixing
203 timescale and therefore would have heterogeneous distributions in the ocean [25].

204 [Linking nutrients, carbon and oxygen](#)

205 Nutrients are linked to oxygen via the limitation of primary production and the associated
206 production and eventual burial of organic carbon, which represents the net source of oxygen – i.e.
207 the net of oxygen production and consumption in respiration and other oxidative pathways. Today
208 plants on land make a major contribution to organic carbon burial and net oxygen production [26],
209 but in the Proterozoic, although there were photosynthetic microbial mats on land [27], they are
210 generally assumed not to have contributed significantly to organic carbon burial. Hence the focus
211 has been on the controls on marine production of organic carbon, its sinking through the water
212 column (the ‘biological pump’), and its preservation and burial in sediments.

213 A crucial notion is that the availability of one nutrient in the ocean ultimately limits the export
214 (sinking) flux of new photosynthetic matter from the surface ocean. Today that nutrient is
215 phosphorus, even though nitrogen may be proximately limiting (i.e. run out first) – because nitrogen
216 levels adjust (on a shorter timescale) to variations in phosphorus levels through the stimulation or

217 suppression of nitrogen fixation (and the action of denitrification) [28, 29]. In the more anoxic
218 Proterozoic-early Paleozoic ocean, we need to consider whether elevated levels of denitrification
219 made nitrogen more proximately limiting (i.e. phosphorus levels in the ocean could considerably
220 exceed organisms' requirement for phosphorus) [25, 30], and whether trace metals limited nitrogen
221 fixation and thus primary production [31].

222 How much of the organic matter created in primary production sinks and reaches the sediments –
223 i.e. the efficiency of the 'biological pump' – plays a crucial role in determining ocean redox state and
224 in setting ocean nutrient levels [4, 16, 25]. On the $\sim 10^3$ yr timescale of ocean mixing, the amount and
225 location of organic matter remineralisation in the water column, together with the supply of oxygen
226 from above, jointly determine the redox state of deeper waters. On the $\sim 10^4$ yr timescale of
227 balancing the phosphorus cycle, the phosphorus (and coupled nitrogen) concentration in the ocean
228 must adjust until output to sediments matches input from rivers. For example, if without complex
229 life the biological pump was less efficient (i.e. it was more difficult to get organic material to the
230 bottom of the shelf seas and ocean and bury it), then (all else being equal) nutrient and productivity
231 levels would need to have been higher to balance the phosphorus cycle [4, 16]. Alternatively, if in a
232 more anoxic ocean there were another efficient way of transferring phosphorus to the sediments –
233 e.g. removal with iron minerals of mixed redox state such as vivianite – then a lower phosphorus
234 concentration could have balanced the phosphorus cycle [32, 33]. Either way, phosphorus
235 concentration can be decoupled from phosphorus input/output.

236 The burial efficiency of organic matter in sediments and the C:P stoichiometry of what is buried also
237 affect phosphorus and atmospheric oxygen levels [34-36]. Today most of the organic material that
238 reaches the sediments is recycled (remineralised) back to the water column. There is a long-running
239 debate about whether organic carbon is more efficiently remineralised under oxic versus anoxic
240 bottom water conditions. Any difference is unclear under the high sedimentation rates of shallow
241 ocean margins where >80% of organic carbon is buried today, but preservation could be markedly

242 more effective under anoxic conditions at the low sedimentation rates in the deep ocean [37]. Under
243 today's oxic ocean conditions, phosphorus is more efficiently recycled than carbon leaving buried
244 organic matter with a higher $(C:P)_{org}$ ratio than primary production, but phosphorus is often trapped
245 in other forms in sediments – especially in authigenic calcium minerals (e.g. apatite), or adsorbed to
246 the surface of iron oxide minerals, meaning the total sedimentary ratio of organic carbon to reactive
247 phosphorus ($C_{org}:P_{react}$) can be lower than in primary production. The recycling of phosphorus from
248 organic matter markedly increases under anoxic conditions, increasing $(C:P)_{org}$ burial ratios,
249 phosphorus concentration, organic carbon burial and atmospheric oxygen [36]. However, if the
250 evolution of complex life increased the efficiency of phosphorus preservation in sediments then this
251 would have lowered phosphorus concentration, organic carbon production and burial and
252 atmospheric oxygen [19].

253 Earth surface redox balance

254 If we tally up all the significant reduced and oxidised reservoirs in the ocean-atmosphere and their
255 input and output fluxes these must be near long-term balance – or Earth's surface redox state,
256 including atmospheric oxygen levels, will change [23, 24]. Today, organic carbon burial is balanced
257 both by the oxidative weathering of ancient sedimentary organic carbon exposed on the continents,
258 and by the volcanic outgassing and subsequent oxidation of subducted organic carbon. The sulphur
259 cycle also plays an important role in today's redox balance. In sediments the electrons in organic
260 carbon may be transferred to pyrite (FeS_2) before burial. Ancient pyrite exposed on the continents is
261 rapidly oxidised and some pyrite sulphur is outgassed and oxidised. Carbon and sulphur also have
262 large oxidised sedimentary reservoirs – carbonate and gypsum – which are deposited from the
263 ocean, weathered on continents and the C and S they contain outgassed from volcanoes following
264 subduction. Over geologic time, the fraction of carbon buried in organic (reduced) versus oxidised
265 form may vary, as may the fraction of sulphur buried in pyrite (reduced) versus oxidised form.
266 Changes in both burial fractions have affected Earth's surface redox state over Phanerozoic time [22,
267 30], but (as will see) the situation was different in the Proterozoic. Furthermore, over Proterozoic

268 timescales, net oxidation of iron in the Earth's crust, and hydrogen loss to space, could have
269 significantly affected Earth surface redox balance.

270 [Alternative model interpretations of proxy data](#)

271 Currently major debates surround oxygen levels in the Proterozoic atmosphere and phosphorus,
272 nitrogen and productivity levels in the Proterozoic ocean. This is partly because different models give
273 very different inferences of key variables from the same proxy data. Summaries of the proxy data
274 can be found in e.g. [25] (spanning Earth history) and [38] (this volume; spanning Neoproterozoic-
275 Paleozoic).

276 [Atmospheric oxygen levels](#)

277 There is currently no widely accepted, direct record of atmospheric oxygen levels prior to the
278 Quaternary ice-core record. Measurements of gas inclusions in halite minerals have been suggested
279 to record the ancient atmosphere [39], but can be contaminated with modern air [40]. Hence
280 attempts to derive a proxy for atmospheric oxygen rely on models. The absence of mass
281 independent fractionation of sulphur isotopes (MIF-S) since the Great Oxidation ~ 2.3 Ga, indicates
282 the continuous presence of an ozone layer and that the sulphate level in the ocean has remained
283 sufficient to prevent any MIF-S signals being recorded. 1-D atmosphere models suggest the ozone
284 layer starts to form at $pO_2 \sim 10^{-5}$ PAL, although total column depth of ozone is still an order of
285 magnitude below present at $pO_2 \sim 0.001$ PAL [41]. The presence of mass independent fractionation
286 of oxygen ($\Delta^{17}O$) at times in the Proterozoic [42], indicates sufficient oxygen and ozone to initiate the
287 required stratospheric photochemistry, which models suggest requires $pO_2 \geq 0.001$ PAL [41, 43].
288 Other proxies for atmospheric oxygen rely on models of oxidation processes in weathering,
289 transport, or shallow ocean environments, which are complicated by the existence of gradients in
290 oxygen concentration from the atmosphere to depth in weathering profiles or shelf seas, and by any
291 presence of organic matter or other reductants.

292 Traditionally, steady state model interpretations of data indicating oxidised iron retention at the top
293 of rare ancient soil profiles (paleosols) were used to set a lower limit on pO_2 , given an assumed pCO_2
294 – e.g. $pO_2 > 0.01$ PAL at 1.85 Ga (Flin Flon paleosol) and at 1.1 Ga (Sturgeon Falls paleosol) [44]. Some
295 subsequent modelling has revised the 1.85 Ga constraint upwards to > 0.05 PAL [45]. Other mass
296 balance modelling has given lower pCO_2 estimates requiring lower pO_2 to explain iron retention [46].
297 Iron retention in the 1.1 Ga Sturgeon Falls paleosol has also been questioned, leaving the 1.1 Ga pO_2
298 inference uncertain [43]. The presence of any microbial mats, e.g. secreting organic acids that can
299 cause iron loss, further complicates paleosol interpretation [27]. More recently, kinetic modelling of
300 abiotic or biotic manganese oxidation and associated chromium oxidation and isotope fractionation
301 was used to argue that $pO_2 < 0.001$ PAL is necessary to explain a lack of positively fractionated $\delta^{53}Cr$
302 in marine ironstones and shales [1]. However, the modelling assumed equilibration of soil pore fluids
303 with atmospheric pO_2 , whereas more realistic 1D modelling of shale weathering shows that the
304 presence of ancient organic matter (kerogen) can readily drive entire weathering profiles anoxic up
305 to $pO_2 \sim 0.05$ PAL [47]. Furthermore, new data has shown evidence of positively fractionated $\delta^{53}Cr$ in
306 mid-Proterozoic shales [48] and carbonates [49] – illustrating that the previous absence of evidence
307 should not have been taken as universal evidence of absence with which to infer pO_2 over > 1 Gyr.
308 Instead it seems likely that pO_2 varied over Proterozoic time. What remains unresolved is what
309 minima it reached when positive $\delta^{53}Cr$ is absent, and whether the overall pattern was of oxygenation
310 events against a very low pO_2 baseline [50], or deoxygenation events against a higher pO_2 baseline.

311 Traditionally, the lack of detrital pyrite (or uraninite) in sediments after the Great Oxidation indicates
312 exposure of these grains to sufficient oxygen in weathering or aquatic transport environments to
313 fully oxidise them. Modelling of shale weathering profiles across observed ranges of erosion rates on
314 the land surface, predicts that the oxidation of pyrite in soils would be incomplete at $pO_2 < 0.1$ PAL
315 [47]. Kinetic modelling of the dissolution of detrital pyrite (and uraninite) grains in solution
316 equilibrated with atmospheric oxygen – e.g. during transport down rivers – indicates $pO_2 > 0.05$ PAL
317 would be required to completely dissolve them, especially for short river transport times [51]. This

318 pO₂ limit would go up if the grains spend time in organic-rich riverine sediments – as seems likely for
319 longer river transport times – because they are readily driven anoxic at low pO₂. These models all
320 depend on poorly known pyrite oxidation kinetics at low pO₂, which have recently been revised
321 faster [52], which will tend to shift the pO₂ lower limits downwards.

322 Deeper ocean redox state

323 Models can indicate how ocean redox state varies with atmospheric pO₂, ocean nutrient levels, and
324 the nature of the biological pump, helping infer ocean redox state from marine sediment proxies.

325 The most established redox proxy – iron speciation of sediments – is a localised proxy usually taken
326 to directly indicate whether overlying waters were oxic, anoxic and sulphate-reducing (euxinic), or
327 anoxic and iron-reducing ('ferruginous'). Models suggest that 'ferruginous' does not imply iron rich,
328 but rather [Fe²⁺] ~0.1μM [25, 53], and oxygen and nitrate rather than iron may dominate organic
329 carbon remineralisation [53]. A growing range of redox-sensitive trace metals with anoxic or euxinic
330 sinks are also being used to try and get a 'global' proxy of ocean redox state. Different metals with
331 different redox sensitivity can add information – for example molybdenum (Mo) removal is
332 specifically sensitive to euxinic (rather than ferruginous) conditions whereas uranium (U) removal
333 tracks anoxic conditions in general. Models are still required to estimate the global spatial extent of
334 anoxic or euxinic bottom waters, and the results are typically sensitive to assumptions about
335 kinetics, the present extent of anoxic bottom waters, and other uncertain terms in the isotopic mass
336 balance. They show that complete removal of redox sensitive metals need not imply global anoxia or
337 euxinia, with estimates of >30-40% of Proterozoic seafloor anoxic and ~1-10% euxinic [54].

338 Consistent with this, basin transects and broader compilations of iron-speciation data indicate a
339 spatially heterogeneous deeper ocean redox state at several Proterozoic times. This is supported by
340 other redox proxies in very rare samples of the deep ocean, which indicate oxic bottom waters at
341 some places and times [55, 56]. To interpret such spatially heterogeneous redox structure requires a
342 spatially explicit model, and one model in particular has been used.

343 GENIE

344 'GENIE' is a coarse-resolution 3-D ocean model coupled to a 2-D (single layer) atmosphere and sea-
345 ice, with marine C, P, S, and optional N, biogeochemical cycling, designed to consider controls on
346 ocean redox state, atmospheric pCO₂ and global temperature. GENIE's strengths include that it is
347 fast for a 3-D model and has data-assimilated modern biogeochemistry, which has been tested
348 against multiple events in the geochemical record. It also captures some of the spatial variability in
349 climate and has an optional weathering module. Key limitations include the lack of an open P cycle,
350 limited iron-nutrient relationships, and very limited resolving of shelf seas. Atmospheric pO₂ is
351 prescribed and so, crucially, is ocean P content. GENIE can be run with a closed or open C cycle
352 (Figure 1) – i.e. with prescribed or interactive pCO₂. With an open C cycle, including interactive
353 silicate weathering, GENIE can be integrated for up to a million years to achieve steady state of the
354 inorganic carbon cycle. However, as ocean P content is prescribed this leads to some timescale
355 inconsistency – e.g. organic carbon burial is prescribed, when in reality it responds interactively (and
356 can affect pCO₂) over such timescales. Hence we concentrate on closed O₂, C and P system
357 applications of GENIE to interpret proxy data, and consider open N system responses. Later we
358 consider the inclusion of ecological dynamics, noting throughout that the lack of an open P cycle
359 response limits what we can infer about dynamical responses over timescales $\geq 10^4$ yr.

360 GENIE has been used to explore how ocean redox state depends on prescribed pO₂ [25, 57], PO₄ [25,
361 58], and the nature of the biological pump [25, 59]. This suggests that spatial redox heterogeneity
362 requires a finely-poised global balance between atmospheric oxygen levels and ocean limiting
363 nutrient levels, and is sensitive to the nature of the biological pump. Assuming a modern biological
364 pump, it requires pO₂:nutrient ~ 0.4 of today's ratio [25], consistent with other models. This can be
365 achieved in very different ways. If Proterozoic pO₂ \ll PAL then nutrients must have been chronically
366 limiting, but if nutrients were near present ocean levels (POL) then pO₂ ~ 0.4 PAL is consistent with
367 times of deeper ocean redox heterogeneity. Prototype inclusion of Fe-S cycling in such a mixed

368 redox state ocean predicts $[\text{Fe}^{2+}] \sim 0.1 \mu\text{M}$ with removal as pyrite in euxinic settings but iron oxide at
369 the oxic-anoxic boundary [25].

370 GENIE further shows that at pO_2 :nutrient < 0.05 of today – under which deeper waters would be
371 completely anoxic – surface waters of the ocean start to exhibit redox heterogeneity including
372 ‘oxygen oases’ and anoxic areas (i.e. they cease to be equilibrated with the atmosphere) [25, 57].

373 This makes other recent model attempts to infer very low $\text{pO}_2 \sim 0.001$ PAL from shallow ocean
374 sediment redox proxies e.g. ~ 1.85 Ga [60] problematic, because conceivably anoxic signatures, e.g.
375 in Ce/Ce* [60] (or iron-speciation), simply indicate anoxic areas caused by excess local reductant
376 input. These may indicate less extreme $\text{pO}_2 < 0.05$ PAL or higher nutrient levels, noting that shallow
377 shelf-sea locations are often enriched with nutrient runoff from land.

378 [Ocean nutrient levels and productivity](#)

379 Modelling was originally used to infer very low ocean $[\text{PO}_4]$ from the phosphorus content of iron
380 formations [61]. Subsequently, experiments showed that the results are highly sensitive to
381 assumptions about the concentration of other ions in seawater, notably silica [62, 63]. Using
382 plausible limits on $[\text{Si}]$, revised estimates put mid-Proterozoic $[\text{PO}_4]$ at or above present ocean levels
383 (POL) and well above them in the Neoproterozoic [64]. A more recent high-profile paper argues from
384 the low bulk phosphorus content of shales that prior to the Neoproterozoic, $[\text{PO}_4] \ll 1$ POL [33].
385 However, the argument that because phosphorus burial was less, phosphorus concentration in the
386 ocean must have been lower is logically flawed. Phosphorus burial is only directly informative of
387 phosphorus input to the ocean (on timescales longer than the residence time), *not* phosphorus
388 concentration. Instead, the authors construct a model (discussed below) in which a very efficient
389 process of phosphorus removal is assumed to have been going on elsewhere, in unrecorded deep
390 ocean settings, thus maintaining low $[\text{PO}_4]$. Without this assumption they predict elevated $[\text{PO}_4]$, and
391 if we assume the biological pump was less efficient, much higher $[\text{PO}_4]$ could be predicted. Hence
392 huge uncertainty currently surrounds Proterozoic $[\text{PO}_4]$ levels. The application of phosphorus

393 speciation to ancient sediments holds great potential to improve knowledge but will also need
394 modelling to interpret it. The first data from ~1 Ga indicates efficient P removal with iron minerals in
395 a low productivity, ferruginous ocean margin setting, but $(C:P)_{org}$ suggests that primary production
396 was no more nutrient limited than today [65].

397 Ancient marine N cycling is hard to constrain even with data and models. The nitrogen isotope
398 composition of shales should provide some information, but unfortunately the same $\delta^{15}N$ signature
399 can be produced in different ways. In GENIE simulations of a mixed redox state Proterozoic ocean,
400 abundant nitrogen fixation comprising $\sim 1/3^{rd}$ of new production is predicted to balance intense
401 regions of denitrification, and the deep ocean comprises small and rapidly turning over reservoirs of
402 nitrate and ammonium in anoxic and oxic waters respectively [25]. Consequently, $[PO_4]$ is decoupled
403 significantly above the nitrogen levels determining productivity and P burial in a more anoxic ocean
404 – at around double the levels that would make it proximately limiting. Recent GENIE results suggests
405 the decoupling of P above N could be even greater [66]. Extending such a spatial model to predict
406 $\delta^{15}N$ distributions could provide a test of this scenario against available data.

407 Recently a simple model has been used to try and infer gross primary productivity (GPP) from the
408 triple oxygen isotope ($\Delta^{17}O$) composition of sedimentary sulphate at particular times in the
409 Proterozoic [42, 67, 68]. However, the problem is under-constrained, because $\Delta^{17}O$ depends jointly
410 on pO_2 , pCO_2 and GPP, with positive correlation between pO_2 and GPP. Hence, e.g. at ~1.4 Ga, both
411 lower pO_2 ~0.001-0.01 PAL and GPP ~6% of today, and higher pO_2 ~0.01-0.1 PAL and GPP ~40% of
412 today, are consistent with the same $\Delta^{17}O$ data [42]. Had the authors considered $pO_2 > 0.1$ PAL their
413 GPP inference would be higher again. The same issue pertains at other times of $\Delta^{17}O$ data, although
414 around ~2 Ga there is $\Delta^{17}O$ evidence that GPP declined [68] or pO_2 increased. Attempts to further
415 constrain the solution space [43], by mechanistically tying the unknown variables together, depend
416 on contestable models (that are discussed next). They risk circular reasoning – taking a model that

417 ties low pO₂ and low nutrients together, taking different model-dependent inferences of low pO₂,
418 and then (unsurprisingly) inferring from $\Delta^{17}\text{O}$ a low productivity, low nutrient, low pO₂ world.

419 Alternative models for global biogeochemical cycling

420 I now consider three recent models of global biogeochemical cycling including oxygen and nutrient
421 levels prior to and during the rise of complex life (Figure 1). I compare and contrast these different
422 models, explain why they come to quite different results, examine what (if any) testable predictions
423 they make, and thus try to establish which (if any) results we should trust. Table 1 summarises and
424 contrasts key process representations in the three models.

425 CANOPS

426 ‘CANOPS’ is a 1-D ocean-atmosphere box model designed to consider controls on ocean nutrient and
427 redox state [69, 70], that has been used to explore how C, N, P, S cycling could have worked under
428 different prescribed levels of atmospheric pO₂ [33, 71]. CANOPS represents several key input and
429 output fluxes from/to the lithosphere, but it does not represent key sedimentary reservoirs or their
430 tectonic cycling. The modelling approach involves prescribing permissible distributions on a range of
431 model boundary conditions (including pO₂), drawing many different instances of the model from
432 those parameter distributions, and running those model variants to steady state for ocean reservoirs
433 (if possible). Additional data-derived constraints may then be imposed on what is considered a
434 permissible result. In ocean steady state, the input/output fluxes do not necessarily balance with
435 respect to particular sedimentary reservoirs, nor do they necessarily achieve redox balance – instead
436 an ad hoc flux is invoked to achieve that [71].

437 In one high-profile publication [33], CANOPS purportedly supports a “stable low-oxygen world” in
438 the Proterozoic with very low ocean nutrient levels. However, as pO₂ is prescribed (by the modellers)
439 the first claim appears tautological. Several critical assumptions in the model’s ocean process
440 representation (Table 1) determine that it produces a low nutrient ocean when low pO₂ is

441 prescribed. Firstly, efficient abiotic removal of phosphorus is prescribed, nominally due to
442 scavenging by iron minerals forming at the redox boundary of a largely anoxic water column
443 (although Fe cycling is not represented). Secondly, the C:P stoichiometry of primary production is
444 assumed to increase ~3-fold under low nutrient levels. Thirdly, organic C preservation is assumed to
445 be more efficient under anoxic conditions [37]. The first assumption directly generates low P and
446 productivity levels. The latter two assumptions dictate that when prescribed low pO_2 inevitably
447 makes the ocean anoxic, in order to match the relatively low organic C content of Proterozoic shales,
448 an anoxic ocean must have low P levels and productivity (because organic carbon creation and
449 preservation are assumed more efficient). Hence the model 'result' is wired into its assumptions. As
450 the authors show [33], if the first assumption is dropped and there is no prescribed efficient
451 scavenging of P, the response to prescribed low pO_2 is completely different, with higher than present
452 P levels in the anoxic ocean supporting greater than present organic carbon burial, which would tend
453 to cause pO_2 to rise.

454 In a subsequent paper [71], CANOPS purportedly manages to "constrain global redox balance",
455 support mid-Proterozoic "severe P biolimitation" and find a role for the sulphur cycle in "regulating
456 atmospheric O_2 levels". Here independent but model-based estimates of $[SO_4] \sim 0.1-1$ mM are used
457 to constrain subsets of permissible model solutions. The modellers show Earth's surface in redox
458 balance by invoking an arbitrary balance term ($\Phi_{out}[Red]$ in Figure 5 of [71] – reproduced here as
459 Figure 2a,b with that flux labelled 'redox imbalance'). However, the failure to impose strict Earth
460 surface redox balance within the model violates the assumption that pO_2 is fixed (stable) and the
461 required balancing flux must be critically examined. Similarly, the lack of balanced sedimentary
462 reservoirs should lead readers to question whether the purported model steady states and assumed
463 pO_2 levels are sustainable in the long-term. In the assumed 'low' $pO_2 \sim 0.001$ PAL case (Figure 2a,
464 reproducing Figure 5a of [71]), the required redox balance term is a large net removal of oxygen (\sim -
465 2.1 Tmol O_2 eq yr^{-1}), which exceeds the sum of the resolved reduced matter input terms (\sim - 1.6 Tmol
466 O_2 eq yr^{-1}), or the uncertainty today in unresolved reduced matter input terms (\sim -($0.8-1.4$) Tmol O_2 eq

467 yr⁻¹). Without this term (i.e. with the fluxes that are actually modelled), pO₂ would tend to rise. With
468 a ~1.1 Tmol O₂ eq yr⁻¹ input of reduced C gases required to balance the organic carbon cycle in the
469 model (and consistent with today's unresolved reduced matter inputs), a ~1 Tmol O₂ eq yr⁻¹
470 imbalance would remain, which can generate today's pO₂ reservoir in 37 Myr. This redox imbalance
471 (and the organic carbon cycle imbalance) largely disappears in CANOPS' 'high' pO₂ ~0.033 PAL case
472 (Figure 2b, reproducing Figure 5b of [71]).

473 The redox imbalance at pO₂ ~0.001 PAL exists because (in electron or oxygen equivalents), pyrite
474 burial greatly exceeds sulphur oxidation, and organic carbon burial far exceeds organic carbon
475 oxidation (plus iron oxidation) requiring a large unresolved input of H₂, CO, CH₄, Fe²⁺. Pyrite
476 oxidation is incomplete, at odds with the lack of detrital pyrite. The imbalance in the S cycle involves
477 an excess of gypsum weathering and (implicit) degassing over (minimal) burial, which is
478 unsustainable over Proterozoic timescales. There was gypsum deposition (for the first time) in the
479 aftermath of the Great Oxidation, but the assumed initial model reservoir of (50±25)×10¹⁸ mol would
480 shrink on a ~100 Myr timescale (based on the modelled input/output imbalance). This would leave a
481 crustal sulphur reservoir dominated by pyrite, invalidating the claim that sulphur cycling and
482 especially pyrite burial played a role in regulating atmospheric O₂ over Proterozoic timescales (see
483 below).

484 'LaaSch'

485 Laakso and Schrag have developed a simple box model – which I dub 'LaaSch' – to consider how
486 atmospheric oxygen could have been regulated at different levels over Earth history [72, 73]. LaaSch
487 is an Earth surface model where outputs have to balance inputs for ocean-atmosphere reservoirs of
488 material to be at steady state. Atmospheric pO₂ is an interactive variable (unlike in CANOPS) and
489 predicting its stable level(s) is a key target of the model. In an early version of LaaSch, C, P, S and
490 alkalinity cycling are included [72], with a subsequent version adding Fe and H cycling [73]. LaaSch
491 does not include sedimentary reservoirs or their tectonic cycling. However, it does require that

492 atmospheric pO_2 and the redox fluxes to/from the surface system adjust until redox balance is
493 achieved. Again one should look at the predicted fluxes into and out from the sediments and
494 consider whether they imply net transfers of C or S (or Fe) between sedimentary forms and whether
495 those are consistent with observations or could be sustained over Proterozoic timescales >100 Myr.

496 In its process representation (Table 1), LaaSCh makes critical assumptions – firstly that phosphorus is
497 increasingly efficiently scavenged by iron minerals in rivers/estuaries as atmospheric pO_2 declines
498 [72]. The shape of the functional response is arbitrarily chosen (and is changed markedly between
499 studies [72, 73]) in a way that generates alternative stable states for atmospheric pO_2 at ~1 PAL and
500 ~0.1 PAL. The authors are explicit that “the parameterization is tuned to give stability [of pO_2] at
501 levels consistent with proxy records”. The reason a decline in P input with declining pO_2 is required is
502 that LaaSCh also assumes spectacularly efficient organic C transfer to sediments in an anoxic water
503 column and very high preservation efficiency in anoxic sediments, which would otherwise tend to
504 push pO_2 back towards modern levels. In a lower Proterozoic pO_2 steady state, LaaSCh simulate only
505 ~0.1% of modern primary production but >70% of it being buried (whereas in today’s world only
506 ~0.1% is buried). Virtually no remineralisation occurs in the model anoxic water column because it is
507 assumed to only depend on O_2 (which is predicted absent) or SO_4 (which has a low predicted
508 concentration), ignoring water column methanogenesis (or other oxidants). This is wrong and
509 demonstrably incompatible with the geochemical record – for example, mid-Proterozoic euxinic
510 shales require a productive biosphere and extensive sulphate reduction, and ignoring water column
511 methanogenesis leads to erroneously low atmospheric methane levels, especially in the Late
512 Archean where there is isotopic evidence for extensive marine methane cycling. The increase in
513 organic carbon burial efficiency under anoxic conditions is also erroneously high because the model
514 only considers the deep ocean, failing to recognise that >80% of organic carbon burial occurs in
515 shallow ocean margin sediments today [74], where the much higher sedimentation rates mask any
516 difference between oxic and anoxic remineralisation rates [37].

517 The modelled 'low O₂' state (Figure 2c) is predominantly stabilised by oxygen-sensitive iron oxidation
518 in the water-column, which would be expected to generate iron deposits and net oxidation of iron in
519 the crust, whereas crustal iron oxidation appears to have mostly occurred during the 'Lomagundi'
520 event 2.22-2.06 Ga [75] and Banded Iron Formations (BIFs) disappeared after ~1.8 Ga. This low pO₂
521 model solution also has gypsum dominating sulphur burial despite pyrite oxidation dominating
522 sulphur input (and that is even true of the Archean "anoxic" model solution, because pyrite
523 oxidation is erroneously assumed to be complete at pO₂ ~10⁻⁷ PAL). This implies a sulphur cycle
524 imbalance with transfer of sulphur from pyrite to gypsum sedimentary reservoirs – and a
525 corresponding carbon cycle imbalance with transfer of electrons from pyrite to the organic carbon
526 sedimentary reservoir. Such a sulphur cycle imbalance is unsustainable over Proterozoic timescales,
527 and is inconsistent with the sporadic nature of gypsum deposition in the Proterozoic and with
528 evidence of widespread anoxic ocean conditions depositing extensive euxinic shales. Furthermore, it
529 is well established from the δ¹³C and δ³⁴S records and from models that do include sedimentary
530 reservoirs that the major transfer of S from pyrite to gypsum (and corresponding transfer of
531 electrons from pyrite to organic carbon) occurred in the Paleozoic [22, 30]. The simulated low pO₂
532 state also has minimal oxidative weathering of organic carbon, because that is wrongly [47] assumed
533 to depend linearly on pO₂ (Table 1). With considerable organic carbon burial this implies massive
534 growth of the sedimentary reservoir of organic carbon over Proterozoic time (Figure 2c). This is a
535 more appropriate scenario for prior to the Great Oxidation than after it [47]. The predicted organic
536 fraction of carbon burial is considerably greater than today, implying higher δ¹³C than the 0‰
537 observed (were it to be simulated). To counter this, the authors invoke an (un-simulated) isotopically
538 heavy authigenic carbonate sink, but authigenic carbonate is typically isotopically light not heavy
539 [76].

540 COPSE

541 My own efforts with colleagues extend the COPSE (Carbon, Oxygen, Phosphorus, Sulphur and
542 Evolution) model, developed and tested for the Phanerozoic [30, 77], back into Proterozoic time [47,
543 78, 79], to try and understand both how the Earth system could have worked and to test hypotheses
544 to establish how it did work. COPSE is an Earth surface model that includes sedimentary rock
545 reservoirs – following the tradition of Garrels, Berner and others. It has not (yet) included material or
546 redox exchange with the mantle (or H loss to space). It maintains ocean-atmosphere redox balance
547 and conserves matter and redox equivalents (electrons) in the total ocean-atmosphere-sediment
548 system. COPSE includes C, O, P, S and N cycling (although some published work has removed the S
549 cycle [47], for reasons explained below). Atmospheric pO_2 is interactive and predicting its stable
550 level(s) is a key model target. COPSE predicts stable isotope records of carbon ($\delta^{13}C$), sulphur ($\delta^{34}S$),
551 and strontium ($^{87}Sr/^{86}Sr$), to enable model testing against data. COPSE is forced by changing solar
552 luminosity, changing tectonic factors (degassing, uplift/erosion), and changing biological factors.

553 Key process representations include a careful treatment of oxidative weathering (of C and S) based
554 on running a detailed 1-D weathering model over a realistic range of erosion rates [47]. This predicts
555 that pyrite oxidation ceases to be complete below $pO_2 \sim 0.1$ PAL, and that organic carbon oxidation
556 ceases at ~ 0.01 PAL and is particularly sensitive to varying pO_2 around ~ 0.1 PAL. COPSE includes the
557 major contribution of land plants to organic carbon burial today, which when removed prior to the
558 mid Paleozoic inevitably produces lower pO_2 and lower $\delta^{13}C \sim 0\%$ (rather than $\sim 2\%$) consistent with
559 data [30]. COPSE does not assume more efficient organic carbon burial under anoxic conditions, but
560 does include more efficient P recycling from organic matter under anoxic conditions, which is well
561 established. It does not invoke more efficient P scavenging under lower pO_2 , either in
562 rivers/estuaries or in an anoxic water column. P fluxes are parameterised based on oxic or euxinic
563 conditions with no special distinction of ferruginous P cycling – because like the other models it does
564 not distinguish euxinic from ferruginous conditions. COPSE includes N cycling but has no distinction

565 of ammonium from nitrate reservoirs, and does not predict $\delta^{15}\text{N}$. The efficiency of the biological
566 pump is not varied. COPSE simulates a predominantly anoxic ocean in the early Paleozoic and
567 preceding Proterozoic, in which N and productivity levels are comparable to modern, but P levels are
568 roughly double modern levels (required to support abundant N-fixation and a balanced N cycle).

569 Proterozoic COPSE simulations with a mostly anoxic ocean predict that pyrite burial dominates S
570 removal and the pyrite sedimentary reservoir dominates the gypsum reservoir. Pyrite oxidation
571 followed by pyrite burial has no net effect on Earth's redox state or atmospheric pO_2 . Hence in one
572 Proterozoic study the S cycle was assumed balanced and removed for simplicity [47]. This contrasts
573 with the (implicitly) unbalanced sulphur cycles of CANOPS (net transfer from gypsum to pyrite) and
574 LaaSch (net transfer from pyrite to gypsum). COPSE predicts stable Proterozoic atmospheric $\text{pO}_2 \sim 0.1$
575 PAL, with a lower limit of $\text{pO}_2 \sim 0.01$ PAL below which the Great Oxidation is reversed because
576 organic carbon burial (electron removal) is insufficient to outweigh the input of reduced volcanic
577 gases that are rapidly oxidised [47]. Incomplete oxidative weathering of organic carbon is the key
578 oxygen regulator and it leads to the robust prediction of stable $\delta^{13}\text{C} \sim 0\text{‰}$, consistent with the long-
579 term record. In a Neoproterozoic study [79], driven by increasing degassing inferred from plate
580 tectonic models, COPSE predicts a modest increase in pO_2 from ~ 0.2 to ~ 0.3 PAL and can reasonably
581 match the $\delta^{34}\text{S}$ and $^{87}\text{Sr}/^{86}\text{Sr}$ records. Subsequent work with COPSE shows how large and persistent
582 Neoproterozoic negative $\delta^{13}\text{C}$ excursions (notably the 'Shuram' event) can be maintained by gypsum
583 evaporite weathering events following earlier sporadic deposition of gypsum [80].

584 [Comparison and evaluation](#)

585 As approaches to understanding how the Proterozoic world could have worked, the three models
586 vary in the timescales they can be applied to (Figure 1). CANOPS (as used thus far) is appropriate for
587 making inferences about shorter timescale variables than pO_2 [33], but inappropriate for considering
588 pO_2 regulation or redox balance over 10+ Myr timescales [71]. LaaSch needs major modifications,
589 after which it may be applied to pO_2 timescales, but not 100+ Myr sedimentary ones [72, 73]. COPSE

590 is applicable to pO_2 and sedimentary timescales but is missing longer timescale exchanges with the
591 mantle. The structural limitations of CANOPS and LaaSCh lead them to predict long-term imbalances
592 in redox [71] and/or crucial elemental cycles [71, 73] that are at odds with data. CANOPS overall has
593 better process representation than LaaSCh, so if its timescale limitations can be overcome (or more
594 carefully considered in study design), it has greater potential.

595 As approaches to establishing how the Proterozoic world actually did work, COPSE makes testable
596 predictions and has successfully simulated key records, notably $\delta^{13}C$. CANOPS qualitatively captures
597 the low organic C content of shales, and LaaSCh discuss the implications of their results for $\delta^{13}C$, but
598 neither CANOPS nor LaaSCh quantitatively predict proxy variables. Hence they cannot test
599 hypotheses (in any quantitative sense).

600 All of the models contain contestable process representations – although at least with COPSE these
601 can (in principle) be falsified if the model fails to match proxy data. COPSE recognises, whilst
602 CANOPS and LaaSCh ignore, the contribution of plants to today's organic carbon burial and oxygen
603 balance. This necessarily generates lower Proterozoic-early Paleozoic pO_2 in COPSE, whereas
604 CANOPS and LaaSCh invoke strong feedbacks to generate bi-stability including an alternative low pO_2
605 steady state. A third option would be that the rise of complex life itself altered pO_2 . To achieve
606 stable low pO_2 , CANOPS assumes very effective P removal with iron minerals to the (anoxic) deep
607 ocean floor, LaaSCh assumes very efficient P removal in rivers/estuaries, but neither of these
608 sedimentary environments tend to be preserved (making these assumptions untestable). COPSE
609 assumes less efficient P removal with iron minerals under anoxic ocean conditions, which warrants
610 revision. CANOPS and LaaSCh also assume organic carbon burial efficiency increases markedly under
611 anoxic conditions, whereas COPSE does not, and the empirical data on this has been widely debated
612 [37].

613 Models linking complex life to biogeochemical cycling

614 There has been less work modelling causal links between complex life and biogeochemical cycling.

615 The hypothesis that the first predatory protists, by grazing on the smallest (cyanobacterial)

616 phytoplankton cells, would have left nutrients underused and thus created a niche for larger (algal)

617 phytoplankton cells [16], is based on adapting a classic model of size-structuring in marine

618 communities [81]. The hypothesis that filter-feeding sponges, by predated the smallest

619 phytoplankton cells, also selected for larger (eukaryotic) algae [4] follows the same logic – although

620 how strong the selective effect of sponges is has yet to be modelled.

621 The same model [81] inspires the hypothesis that putative extreme Proterozoic nutrient limitation

622 could have limited phytoplankton cell size and the expansion of eukaryotic algae [7]. Recent

623 inclusion of a size-structured marine ecosystem in GENIE [82], confirms the original results [81] that

624 prescribed nutrients limit cell size and trophic structure – for example, excluding zooplankton if PO_4

625 <10% of present ocean levels [82]. However, if GENIE had an open phosphorus cycle, the

626 correspondingly weak biological pump and limited P supply to sediments should cause ocean $[\text{PO}_4]$

627 to rise and rebalance at a higher concentration. Furthermore, the most abundant algae in today's

628 ocean are 1-3 μm diameter mixotrophs that predate cyanobacteria [83] and would not be excluded

629 even at 1% of present ocean nutrient levels [82]. Hence the hypothesis that lack of nutrients

630 prevented the expansion of marine algae lacks support from current models.

631 Whilst CANOPS assumes the biological pump has got less efficient since the mid-Proterozoic, LaaSCh

632 assumes it has got much less efficient, and COPSE assumes no change in efficiency, other models

633 have begun to examine the effects of postulated increases in the efficiency of the biological pump

634 [4, 14]. Effects on ocean redox structure have been considered independently of effects on

635 phosphorus levels, but over $>10^4$ yr timescales these effects should be consistently combined [4, 16].

636 3D GENIE simulations of effects on redox structure for a prescribed ocean nutrient inventory, show
637 that without an effective biological pump, diffusion concentrates oxygen demand in intermediate
638 waters just below the surface ocean, generating the most intense anoxia there [25]. This could have
639 left the deep ocean oxygenated by ventilation from high latitude surface waters, thanks to little or
640 no oxygen demand from organic matter – assuming $pO_2 > 0.001$ PAL and 20 Sv ventilation sufficient
641 to outweigh abiotic reductant input from mid-ocean ridges [25]. An inefficient biological pump also
642 makes it harder to drive the deeper parts of shelf seas anoxic. As the biological pump becomes more
643 efficient, this shifts oxygen demand to deeper waters and sediments, making it easier to drive deep
644 shelves and the deep ocean anoxic, but making it harder to drive (near) surface waters anoxic.

645 However, the effect of changes in the biological pump on ocean P inventory (over $\sim 10^4$ yr timescales)
646 and hence total oxygen demand in the water column works in the opposite direction. Simple
647 calculations suggest going from cyanobacterial to algal cells causes a roughly 10-fold increase in
648 sinking terminal velocity and a 2.5-fold increase in material reaching the sediments [84]. A less
649 efficient biological pump requires higher limiting nutrient levels in order to balance the P cycle, and
650 an increase in pump efficiency tends to lower those nutrient levels, thus lowering total oxygen
651 demand in the water column. Simple modelling of the net effect supports earlier suppositions [4,
652 16] that the change in nutrient inventory dominates – with a weaker pump P levels are higher and
653 therefore deep anoxia more intense. As the pump strengthens this tends to lower ocean P levels and
654 the propensity for anoxia. The (much) longer timescale effects on organic C burial and atmospheric
655 pO_2 may work in the opposite direction again: if C_{org}/P_{react} burial ratios decline with ocean
656 oxygenation this will cause pO_2 to decline, ultimately reinstating anoxia, and creating the potential
657 for long-timescale oscillations [85, 86]. Other modelling predicts that an increase in biological pump
658 efficiency lowered atmospheric pCO_2 and might have contributed to triggering snowball Earth events
659 [87].

660 Models have yet to simulate the impact of sessile benthic animals including sponges and
661 'rangeomorph' fronds concentrating resources where they were located on the sediments [17].
662 However, models have begun to consider proposed impacts of mobile, burrowing, bioturbating
663 animals on biogeochemical cycling [18, 19]. Including in COPSE the idea that by oxygenating the
664 upper sediments, bioturbating animals increase the retention of phosphorus and lower the $(C/P)_{org}$
665 burial ratio, leads to a decline and then stabilisation of atmospheric pO_2 , consistent with evidence of
666 ocean deoxygenation in the Late Cambrian-Ordovician [19]. The assumed timing of significant
667 increase in bioturbation depth has been critiqued and argued to be much later in the Paleozoic [88].
668 However, a subsequent version of COPSE showed that an early, non-linear impact of shallow
669 burrowing on C, S and P sediment cycling provides a better fit to $\delta^{13}C$, $\delta^{34}S$ and ocean redox data
670 than a late impact [89]. Alongside this simple box modelling, detailed 1D reaction-transport
671 sediment modelling has provided some support that bioturbation lowers C_{org}/P_{react} burial ratios [90].
672 There is clearly scope for more detailed process modelling of this kind to generate further insight
673 into effects of bioturbation on P-speciation.

674 Ways forward

675 There is considerable scope for improved Proterozoic biogeochemical modelling. Better models of
676 weathering, transport and sedimentary environments can improve understanding and interpretation
677 of proxies. Models of global biogeochemical cycling need to be built on well-established principles,
678 incorporating appropriate reservoirs and processes for the timescales they pertain to address –
679 which for considerations of atmospheric oxygen regulation means enforcing Earth's surface redox
680 balance and including sedimentary reservoirs. Biogeochemical models should predict proxy data
681 targets to be testable and adding proxy targets has the potential to constrain model results – for
682 example, COPSE could predict $\Delta^{17}O$ and better predict P-speciation. Once an appropriate model
683 structure and link to data is established, a key unsolved challenge is to establish whether and how
684 atmospheric oxygen could be regulated at $pO_2 \sim 0.001$ PAL. Predicting long-term fluctuations in pO_2

685 and nutrient levels is also a key target, which will require reconstruction of tectonic drivers and
686 representation of how they affect climate and weathering.

687 Biogeochemical modelling should also explore a wider ‘possibility space’ of process assumptions.

688 Most existing models assume phosphorus is the ultimate limiting nutrient, although COPSE and
689 GENIE find nitrogen much more proximately limiting when anoxia is widespread, suggesting that
690 possible trace metal limitation of nitrogen fixation deserves consideration [31]. Current models also
691 assume that marine phytoplankton dominated global primary production in the Proterozoic, but if
692 we take seriously existing predictions of much lower phytoplankton productivity [33, 71, 73, 84, 91],
693 then modelling should consider whether microbial mats at the bottom of shelf-seas, in freshwaters
694 and/or on land [27] could have contributed significantly to global productivity. More complete Earth
695 system modelling, including other potentially important factors for complex life, notably climate and
696 the occurrence of ‘snowball Earth’ events, would also add insight and constraint results.

697 The possibility of significant feedback between biogeochemical conditions and the rise of complex
698 life invites approaches that go beyond biogeochemical modelling. Trait-based physiological and
699 ecological modelling could capture the environmental constraints on particular types of complex life,
700 and coupling this to biogeochemical modelling could capture resultant feedbacks. For example,
701 models of the physiological constraints on sponge pumping metabolism [92] and its hydrodynamics
702 [93], could be coupled to models of its effects on phytoplankton community size structure and
703 biogeochemical cycling. Size-structured modelling of phytoplankton community dynamics [81, 82]
704 could be extended to model the effects of different cell sizes, faecal pellets, zooplankton vertical
705 migration, etcetera, on the biological pump [94-96], and resultant biogeochemical feedbacks. This
706 more comprehensive approach would offer new opportunities for testing hypotheses against
707 empirical data. For example, the combination of molecular phylogenetics and relaxed molecular
708 clocks calibrated on minimum ages from fossils can provide timing estimates for the origin of
709 particular traits (e.g. animal guts). Models that can map from these traits to their biogeochemical

710 consequences, including observable proxies, then give the potential to test and refine those age
711 estimates.

712 Summary and implications

713 Some of the disagreements between existing models of atmospheric oxygen and ocean nutrient
714 levels associated with the rise of complex life are the result of applying conceptual frameworks
715 designed for a shorter range of timescales to longer timescales and questions, which demand the
716 consideration of additional processes and balances. Some are due to disagreement over uncertain
717 process representations, and some are due to clear flaws in process representation in some models.

718 Considering these model limitations, I conclude that Proterozoic atmospheric pO_2 varying in the
719 range ~ 0.01 - 0.4 PAL is mechanistically plausible and could be consistent with available proxies,
720 depending on the timing of pO_2 variations. No consistent model of biogeochemical cycling yet shows
721 how pO_2 could be regulated at ≤ 0.001 PAL over long timescales, and it is not clear from model
722 interpretations that any proxy demands such low levels, if we recognise that reductant inputs can
723 create disequilibrium anoxic conditions in near-surface environments. However, this does not rule
724 out that such conditions occurred and it should inspire further modelling to see if and how they
725 could occur. Meanwhile, given current estimates of their minimum oxygen requirements it is unclear
726 that the evolution of stem group animals, sponges, or simple bilaterian animals was prevented by
727 lack of oxygen. However, the same reductant input that can create local anoxia and anoxic proxy
728 signatures would clearly pose a problem for animals in those local environments. Furthermore, it
729 remains possible that insufficient pO_2 and/or unstable redox conditions restricted the later rise of
730 more oxygen-demanding animal traits and modes of life.

731 A very wide range of stable Proterozoic phosphorus levels and associated productivity could be
732 consistent with available phosphorus burial data, depending on contestable and largely untested
733 model assumptions. Furthermore, phosphorus levels could have been several times above Redfield

734 ratio to proximately limiting nitrogen levels in a largely anoxic ocean. The lower atmospheric pO_2 ,
735 the lower the limiting nutrient level consistent with times of heterogeneous ocean redox structure,
736 but Earth surface redox balance requires a marine organic carbon burial flux of comparable order-of-
737 magnitude to today. This makes it crucial to resolve the efficiency of the biological pump prior to
738 complex life and the efficiency of organic carbon remineralisation in a more anoxic ocean. Until we
739 have more P-speciation data and models tested against it, the jury should remain out on Proterozoic
740 nutrient levels. Currently there is no decisive support for nutrient limitation of algae prior to the
741 Cryogenian, leaving the late rise of algae to ecological prominence as an unsolved puzzle.

742 The effects of complex life on biogeochemical cycling remain wide open for exploration, with current
743 models suggesting that they could be substantial.

744 Author contributions

745 TML conceived the study, analysed the different models, and wrote the paper.

746 Acknowledgements

747 I thank Jochen Brocks for asking probing questions about the use of models, Stuart Daines and
748 Richard Boyle for valuable input, fellow organisers and participants of the Royal Society Discussion
749 and Satellite meetings for stimulating discussions, and two anonymous referees for positive
750 feedback that improved the paper.

751 Data accessibility

752 All data discussed were extracted from the cited literature and can be found there.

753 Funding

754 This work was supported by the Natural Environment Research Council, through the Biosphere
755 Evolution, Transitions and Resilience programme (grant number NE/P013651/1).

756 **References**

- 757 [1] Planavsky, N.J., Reinhard, C.T., Wang, X., Thomson, D., McGoldrick, P., Rainbird, R.H., Johnson, T.,
758 Fischer, W.W. & Lyons, T.W. 2014 Low Mid-Proterozoic atmospheric oxygen levels and the delayed
759 rise of animals. *Science* **346**, 635-638. (doi:10.1126/science.1258410).
- 760 [2] Sperling, E.A., Frieder, C.A., Raman, A.V., Girguis, P.R., Levin, L.A. & Knoll, A.H. 2013 Oxygen,
761 ecology, and the Cambrian radiation of animals. *Proceedings of the National Academy of Sciences*
762 **110**, 13446-13451. (doi:10.1073/pnas.1312778110).
- 763 [3] Butterfield, N.J. 2009 Oxygen, animals and oceanic ventilation: an alternative view. *Geobiology* **7**,
764 1-7. (doi:10.1111/j.1472-4669.2009.00188.x).
- 765 [4] Lenton, T.M., Boyle, R.A., Poulton, S.W., Shields, G.A. & Butterfield, N.J. 2014 Co-evolution of
766 eukaryotes and ocean oxygenation in the Neoproterozoic era. *Nature Geoscience* **7**, 257-265.
767 (doi:10.1038/ngeo2108).
- 768 [5] Davidson, E.H. & Erwin, D.H. 2006 Gene Regulatory Networks and the Evolution of Animal Body
769 Plans. *Science* **311**, 796-800. (doi:10.1126/science.1113832).
- 770 [6] Boyle, R.A., Lenton, T.M. & Williams, H.T.P. 2007 Neoproterozoic 'snowball Earth' glaciations and
771 the evolution of altruism. *Geobiology* **5**, 337-349. (doi:10.1111/j.1472-4669.2007.00115.x).
- 772 [7] Brocks, J.J., Jarrett, A.J.M., Sirantoine, E., Hallmann, C., Hoshino, Y. & Liyanage, T. 2017 The rise of
773 algae in Cryogenian oceans and the emergence of animals. *Nature* **548**, 578-581.
774 (doi:10.1038/nature23457).
- 775 [8] Nursall, J.R. 1959 Oxygen as a prerequisite to the origin of the Metazoa. *Nature* **183**, 1170-1172.
- 776 [9] Mills, D.B., Ward, L.M., Jones, C., Sweeten, B., Forth, M., Treusch, A.H. & Canfield, D.E. 2014
777 Oxygen requirements of the earliest animals. *Proceedings of the National Academy of Sciences* **111**,
778 14168-4172. (doi:10.1073/pnas.1400547111).
- 779 [10] Sperling, E.A., Knoll, A.H. & Girguis, P.R. 2015 The Ecological Physiology of Earth's Second
780 Oxygen Revolution. *Annual Review of Earth and Planetary Sciences* **46**, 215-235.

- 781 [11] Poulton, S.W., Fralick, P.W. & Canfield, D.E. 2010 Spatial variability in oceanic redox structure
782 1.8-billion years ago. *Nature Geosci* **3**, 486-490.
- 783 [12] Maynard Smith, J. & Szathmáry, E. 1995 *The Major Transitions in Evolution*. Oxford, Freeman.
- 784 [13] Okasha, S. 2006 *Evolution and the Levels of Selection*. Oxford, Oxford University Press.
- 785 [14] Logan, G.B., Hayes, J.M., Hieshima, G.B. & Summons, R.E. 1995 Terminal Proterozoic
786 reorganization of biogeochemical cycles. *Nature* **376**, 53-56.
- 787 [15] Butterfield, N.J. 2011 Animals and the invention of the Phanerozoic Earth system. *Trends in*
788 *Ecology & Evolution* **26**, 81-87.
- 789 [16] Lenton, T.M. & Daines, S.J. 2018 The effects of marine eukaryote evolution on phosphorus,
790 carbon and oxygen cycling across the Proterozoic-Phanerozoic transition. *Emerging Topics in Life*
791 *Sciences*, ETLS20170156. (doi:10.1042/ETLS20170156).
- 792 [17] Budd, G.E. & Jensen, S. 2017 The origin of the animals and a 'Savannah' hypothesis for early
793 bilaterian evolution. *Biological Reviews* **92**, 446-473. (doi:10.1111/brv.12239).
- 794 [18] Canfield, D.E. & Farquhar, J. 2009 Animal evolution, bioturbation, and the sulfate concentration
795 of the oceans. *Proceedings of the National Academy of Sciences* **106**, 8123-8127.
796 (doi:10.1073/pnas.0902037106).
- 797 [19] Boyle, R.A., Dahl, T.W., Dale, A.W., Shields-Zhou, G.A., Zhu, M., Brasier, M.D., Canfield, D.E. &
798 Lenton, T.M. 2014 Stabilization of the coupled oxygen and phosphorus cycles by the evolution of
799 bioturbation. *Nature Geoscience* **7**, 671-676. (doi:10.1038/ngeo2213).
- 800 [20] Kump, L.R. 1989 Chemical Stability of the Atmosphere and Ocean. *Palaeogeography,*
801 *Palaeoclimatology, Palaeoecology (Global and Planetary Change Section)* **75**, 123-136.
- 802 [21] Hayes, J.M. & Waldbauer, J.R. 2006 The carbon cycle and associated redox processes through
803 time. *Phil. Trans. B* **361**, 931-950.
- 804 [22] Garrels, R.M. & Lerman, A. 1981 Phanerozoic cycles of sedimentary carbon and sulfur.
805 *Proceedings of the National Academy of Sciences USA* **78**, 4652-4656.

- 806 [23] Garrels, R.M., Lerman, A. & Mackenzie, F.T. 1976 Controls of Atmospheric O₂ and CO₂: Past,
807 Present, and Future. *American Scientist* **64**, 306-315.
- 808 [24] Garrels, R.M. & Perry, E.A., Jr. 1974 Cycling of carbon, sulfur, and oxygen through geologic time.
809 In *The Sea* (pp. 303-336. New York, Wiley).
- 810 [25] Lenton, T.M. & Daines, S.J. 2017 Biogeochemical Transformations in the History of the Ocean.
811 *Annual Review of Marine Science* **9**, 31-58. (doi:10.1146/annurev-marine-010816-060521).
- 812 [26] Burdige, D.J. 2005 Burial of terrestrial organic matter in marine sediments: A re-assessment.
813 *Global Biogeochemical Cycles* **19**, n/a-n/a. (doi:10.1029/2004GB002368).
- 814 [27] Lenton, T.M. & Daines, S.J. 2017 Matworld – the biogeochemical effects of early life on land.
815 *New Phytologist* **215**, 531-537. (doi:doi:10.1111/nph.14338).
- 816 [28] Tyrrell, T. 1999 The relative influences of nitrogen and phosphorus on oceanic primary
817 production. *Nature* **400**, 525-531.
- 818 [29] Lenton, T.M. & Watson, A.J. 2000 Redfield revisited: 1. Regulation of nitrate, phosphate and
819 oxygen in the ocean. *Global Biogeochemical Cycles* **14**, 225-248.
- 820 [30] Lenton, T.M., Daines, S.J. & Mills, B.J.W. 2018 COPSE reloaded: An improved model of
821 biogeochemical cycling over Phanerozoic time. *Earth Science Reviews* **178**, 1-28.
- 822 [31] Anbar, A.D. & Knoll, A.H. 2002 Proterozoic Ocean Chemistry and Evolution: A Bioinorganic
823 Bridge? *Science* **297**, 1137-1142.
- 824 [32] Derry, L.A. 2015 Causes and consequences of mid-Proterozoic anoxia. *Geophysical Research*
825 *Letters* **42**, 8538-8546. (doi:10.1002/2015GL065333).
- 826 [33] Reinhard, C.T., Planavsky, N.J., Gill, B.C., Ozaki, K., Robbins, L.J., Lyons, T.W., Fischer, W.W.,
827 Wang, C., Cole, D.B. & Konhauser, K.O. 2016 Evolution of the global phosphorus cycle. *Nature* **541**,
828 386-389. (doi:10.1038/nature20772).
- 829 [34] Betts, J.N. & Holland, H.D. 1991 The oxygen content of ocean bottom waters, the burial
830 efficiency of organic carbon, and the regulation of atmospheric oxygen. *Palaeogeography,*
831 *Palaeoclimatology, Palaeoecology (Global and Planetary Change Section)* **97**, 5-18.

- 832 [35] Van Cappellen, P. & Ingall, E.D. 1994 Benthic phosphorus regeneration, net primary production,
833 and ocean anoxia: A model of the coupled marine biogeochemical cycles of carbon and phosphorus.
834 *Paleoceanography* **9**, 677-692.
- 835 [36] Van Cappellen, P. & Ingall, E.D. 1996 Redox stabilisation of the Atmosphere and Oceans by
836 Phosphorus-Limited Marine Productivity. *Science* **271**, 493-496.
- 837 [37] Katsev, S. & Crowe, S.A. 2015 Organic carbon burial efficiencies in sediments: The power law of
838 mineralization revisited. *Geology* **43**, 607-610. (doi:10.1130/g36626.1).
- 839 [38] Tostevin, R. & Mills, B.J.W. 2020 Reconciling proxy records and models of Earth's oxygenation
840 during the Neoproterozoic and Paleozoic. *Royal Society Interface Focus*, in press.
- 841 [39] Blamey, N.J.F., Brand, U., Parnell, J., Spear, N., Lécuyer, C., Benison, K., Meng, F. & Ni, P. 2016
842 Paradigm shift in determining Neoproterozoic atmospheric oxygen. *Geology* **44**, 651-654.
843 (doi:10.1130/g37937.1).
- 844 [40] Yeung, L.Y. 2017 Low oxygen and argon in the Neoproterozoic atmosphere at 815 Ma. *Earth and*
845 *Planetary Science Letters* **480**, 66-74. (doi:10.1016/j.epsl.2017.09.044).
- 846 [41] Segura, A., Krelow, K., Kasting, J.F., Sommerlatt, D., Meadows, V., Crisp, D., Cohen, M. &
847 Mlawer, E. 2003 Ozone Concentrations and Ultraviolet Fluxes on Earth-Like Planets Around Other
848 Stars. *Astrobiology* **3**, 689-708. (doi:10.1089/153110703322736024).
- 849 [42] Crockford, P.W., Hayles, J.A., Bao, H., Planavsky, N.J., Bekker, A., Fralick, P.W., Halverson, G.P.,
850 Bui, T.H., Peng, Y. & Wing, B.A. 2018 Triple oxygen isotope evidence for limited mid-Proterozoic
851 primary productivity. *Nature* **559**, 613-616. (doi:10.1038/s41586-018-0349-y).
- 852 [43] Planavsky, N.J., Cole, D.B., Isson, T.T., Reinhard, C.T., Crockford, P.W., Sheldon, N.D. & Lyons,
853 T.W. 2018 A case for low atmospheric oxygen levels during Earth's middle history. *Emerging Topics*
854 *in Life Sciences* **2**, 149-159. (doi:10.1042/etls20170161).
- 855 [44] Rye, R. & Holland, H.D. 1998 Paleosols and the evolution of atmospheric oxygen: A critical
856 review. *American Journal of Science* **298**, 621-672.

- 857 [45] Yokota, K., Kanzaki, Y. & Murakami, T. 2013 Weathering model for the quantification of
858 atmospheric oxygen evolution during the Paleoproterozoic. *Geochimica et Cosmochimica Acta* **117**,
859 332-347. (doi:10.1016/j.gca.2013.03.015).
- 860 [46] Sheldon, N.D. 2006 Precambrian paleosols and atmospheric CO₂ levels. *Precambrian Research*
861 **147**, 148-155.
- 862 [47] Daines, S.J., Mills, B. & Lenton, T.M. 2017 Atmospheric oxygen regulation at low Proterozoic
863 levels by incomplete oxidative weathering of sedimentary organic carbon. *Nature Communications*
864 **8**, 14379. (doi:10.1038/ncomms14379).
- 865 [48] Canfield, D.E., Zhang, S., Frank, A.B., Wang, X., Wang, H., Su, J., Ye, Y. & Frei, R. 2018 Highly
866 fractionated chromium isotopes in Mesoproterozoic-aged shales and atmospheric oxygen. *Nature*
867 *Communications* **9**, 2871. (doi:10.1038/s41467-018-05263-9).
- 868 [49] Gilleaudeau, G.J., Frei, R., Kaufman, A.J., Kah, L.C., Azmy, K., Bartley, J.K., Chernyavskiy, P. &
869 Knoll, A.H. 2016 Oxygenation of the mid-Proterozoic atmosphere: clues from chromium isotopes in
870 carbonates. *Geochemical Perspectives Letters* **2**, 178-187. (doi:10.7185/geochemlet.1618).
- 871 [50] Diamond, C.W. & Lyons, T.W. 2018 Mid-Proterozoic redox evolution and the possibility of
872 transient oxygenation events. *Emerging Topics in Life Sciences* **2**, 235-245.
873 (doi:10.1042/etls20170146).
- 874 [51] Johnson, J.E., Gerpheide, A., Lamb, M.P. & Fischer, W.W. 2014 O₂ constraints from
875 Paleoproterozoic detrital pyrite and uraninite. *Geological Society of America Bulletin* **126**, 813-830.
876 (doi:10.1130/b30949.1).
- 877 [52] Johnson, A.C., Romaniello, S.J., Reinhard, C.T., Gregory, D.D., Garcia-Robledo, E., Revsbech, N.P.,
878 Canfield, D.E., Lyons, T.W. & Anbar, A.D. 2019 Experimental determination of pyrite and
879 molybdenite oxidation kinetics at nanomolar oxygen concentrations. *Geochimica et Cosmochimica*
880 *Acta* **249**, 160-172. (doi:10.1016/j.gca.2019.01.022).

- 881 [53] Wallmann, K., Flögel, S., Scholz, F., Dale, A.W., Kemena, T.P., Steinig, S. & Kuhnt, W. 2019
882 Periodic changes in the Cretaceous ocean and climate caused by marine redox see-saw. *Nature*
883 *Geoscience* **12**, 456-461. (doi:10.1038/s41561-019-0359-x).
- 884 [54] Reinhard, C.T., Planavsky, N.J., Robbins, L.J., Partin, C.A., Gill, B.C., Lalonde, S.V., Bekker, A.,
885 Konhauser, K.O. & Lyons, T.W. 2013 Proterozoic ocean redox and biogeochemical stasis. *Proceedings*
886 *of the National Academy of Sciences* **110**, 5357-5362. (doi:10.1073/pnas.1208622110).
- 887 [55] Slack, J.F., Grenne, T. & Bekker, A. 2009 Seafloor-hydrothermal Si-Fe-Mn exhalites in the Pecos
888 greenstone belt, New Mexico, and the redox state of ca. 1720 Ma deep seawater. *Geosphere* **5**, 302-
889 314. (doi:10.1130/ges00220.1).
- 890 [56] Slack, J.F., Grenne, T., Bekker, A., Rouxel, O.J. & Lindberg, P.A. 2007 Suboxic deep seawater in
891 the late Paleoproterozoic: Evidence from hematitic chert and iron formation related to seafloor-
892 hydrothermal sulfide deposits, central Arizona, USA. *Earth and Planetary Science Letters* **255**, 243-
893 256.
- 894 [57] Reinhard, C.T., Planavsky, N.J., Olson, S.L., Lyons, T.W. & Erwin, D.H. 2016 Earth's oxygen cycle
895 and the evolution of animal life. *Proceedings of the National Academy of Sciences* **113**, 8933-8938.
896 (doi:10.1073/pnas.1521544113).
- 897 [58] Monteiro, F.M., Pancost, R.D., Ridgwell, A. & Donnadieu, Y. 2012 Nutrients as the dominant
898 control on the spread of anoxia and euxinia across the Cenomanian-Turonian oceanic anoxic event
899 (OAE2): Model-data comparison. *Paleoceanography* **27**, PA4209. (doi:10.1029/2012PA002351).
- 900 [59] Meyer, K.M., Ridgwell, A. & Payne, J.L. 2016 The influence of the biological pump on ocean
901 chemistry: implications for long-term trends in marine redox chemistry, the global carbon cycle, and
902 marine animal ecosystems. *Geobiology* **14**, 207-219. (doi:10.1111/gbi.12176).
- 903 [60] Bellefroid, E.J., Hood, A.v.S., Hoffman, P.F., Thomas, M.D., Reinhard, C.T. & Planavsky, N.J. 2018
904 Constraints on Paleoproterozoic atmospheric oxygen levels. *Proceedings of the National Academy of*
905 *Sciences* **115**, 8104-8109. (doi:10.1073/pnas.1806216115).

- 906 [61] Bjerrum, C.J. & Canfield, D.E. 2002 Ocean productivity before about 1.9 Gyr ago limited by
907 phosphorus adsorption onto iron oxides. *Nature* **417**, 159-162.
- 908 [62] Konhauser, K.O., Lalonde, S.V., Amskold, L. & Holland, H.D. 2007 Was There Really an Archean
909 Phosphate Crisis? *Science* **315**, 1234-1234. (doi:10.1126/science.1136328).
- 910 [63] Jones, C., Nomosatryo, S., Crowe, S.A., Bjerrum, C.J. & Canfield, D.E. 2015 Iron oxides, divalent
911 cations, silica, and the early earth phosphorus crisis. *Geology*. (doi:10.1130/g36044.1).
- 912 [64] Planavsky, N.J., Rouxel, O.J., Bekker, A., Lalonde, S.V., Konhauser, K.O., Reinhard, C.T. & Lyons,
913 T.W. 2010 The evolution of the marine phosphate reservoir. *Nature* **467**, 1088-1090.
- 914 [65] Guilbaud, R., Poulton, S.W., Thompson, J., Husband, K.F., Zhu, M., Zhou, Y., Shields, G.A. &
915 Lenton, T.M. 2020 Phosphorus-limited conditions in the early Neoproterozoic ocean maintained low
916 levels of atmospheric oxygen. *Nature Geoscience* **13**, 296-301.
- 917 [66] Naafs, B.D.A., Monteiro, F.M., Pearson, A., Higgins, M.B., Pancost, R.D. & Ridgwell, A. 2019
918 Fundamentally different global marine nitrogen cycling in response to severe ocean deoxygenation.
919 *Proceedings of the National Academy of Sciences* **116**, 24979-24984.
920 (doi:10.1073/pnas.1905553116).
- 921 [67] Crockford, P.W., Kunzmann, M., Bekker, A., Hayles, J., Bao, H., Halverson, G.P., Peng, Y., Bui,
922 T.H., Cox, G.M., Gibson, T.M., et al. 2019 Claypool continued: Extending the isotopic record of
923 sedimentary sulfate. *Chemical Geology* **513**, 200-225. (doi:10.1016/j.chemgeo.2019.02.030).
- 924 [68] Hodgskiss, M.S.W., Crockford, P.W., Peng, Y., Wing, B.A. & Horner, T.J. 2019 A productivity
925 collapse to end Earth's Great Oxidation. *Proceedings of the National Academy of Sciences* **116**,
926 17207-17212. (doi:10.1073/pnas.1900325116).
- 927 [69] Ozaki, K. & Tajika, E. 2013 Biogeochemical effects of atmospheric oxygen concentration,
928 phosphorus weathering, and sea-level stand on oceanic redox chemistry: Implications for
929 greenhouse climates. *Earth and Planetary Science Letters* **373**, 129-139.
930 (doi:10.1016/j.epsl.2013.04.029).

- 931 [70] Ozaki, K., Tajima, S. & Tajika, E. 2011 Conditions required for oceanic anoxia/euxinia: Constraints
932 from a one-dimensional ocean biogeochemical cycle model. *Earth and Planetary Science Letters* **304**,
933 270-279.
- 934 [71] Ozaki, K., Reinhard, C.T. & Tajika, E. 2019 A sluggish mid-Proterozoic biosphere and its effect on
935 Earth's redox balance. *Geobiology* **17**, 3-11. (doi:10.1111/gbi.12317).
- 936 [72] Laakso, T.A. & Schrag, D.P. 2014 Regulation of atmospheric oxygen during the Proterozoic. *Earth*
937 *and Planetary Science Letters* **388**, 81-91. (doi:10.1016/j.epsl.2013.11.049).
- 938 [73] Laakso, T.A. & Schrag, D.P. 2017 A theory of atmospheric oxygen. *Geobiology* **15**, 366-384.
939 (doi:10.1111/gbi.12230).
- 940 [74] Burdige, D.J. 2007 Preservation of Organic Matter in Marine Sediments: Controls, Mechanisms,
941 and an Imbalance in Sediment Organic Carbon Budgets? *Chemical Reviews* **107**, 467-485.
942 (doi:10.1021/cr050347q).
- 943 [75] Bekker, A. & Holland, H.D. 2012 Oxygen overshoot and recovery during the early
944 Paleoproterozoic. *Earth and Planetary Science Letters* **317-318**, 295-304.
945 (doi:10.1016/j.epsl.2011.12.012).
- 946 [76] Naehr, T.H., Eichhubl, P., Orphan, V.J., Hovland, M., Paull, C.K., Ussler, W., Lorenson, T.D. &
947 Greene, H.G. 2007 Authigenic carbonate formation at hydrocarbon seeps in continental margin
948 sediments: A comparative study. *Deep Sea Research Part II: Topical Studies in Oceanography* **54**,
949 1268-1291. (doi:10.1016/j.dsr2.2007.04.010).
- 950 [77] Bergman, N.M., Lenton, T.M. & Watson, A.J. 2004 COPSE: a new model of biogeochemical
951 cycling over Phanerozoic time. *Am. J. Sci.* **304**, 397-437.
- 952 [78] Mills, B., Lenton, T.M. & Watson, A.J. 2014 Proterozoic oxygen rise linked to shifting balance
953 between seafloor and terrestrial weathering. *PNAS* **111**, 9073-9078.
954 (doi:10.1073/pnas.1321679111).
- 955 [79] Williams, J.J., Mills, B.J.W. & Lenton, T.M. 2019 A tectonically-driven Ediacaran oxygenation
956 event. *Nature Communications* **10**, 2690.

- 957 [80] Shields, G.A., Mills, B.J.W., Zhu, M., Raub, T.D., Daines, S.J. & Lenton, T.M. 2019 Unique
958 Neoproterozoic carbon isotope excursions sustained by coupled evaporite dissolution and pyrite
959 burial. *Nature Geoscience* **12**, 823-827. (doi:10.1038/s41561-019-0434-3).
- 960 [81] Armstrong, R.A. 1994 Grazing limitation and nutrient limitation in marine ecosystems: Steady
961 state solutions of an ecosystem model with multiple food chains. *Limnology and Oceanography* **39**,
962 597-608. (doi:10.4319/lo.1994.39.3.0597).
- 963 [82] Reinhard, C.T., Planavsky, N.J., Ward, B.A., Love, G.D., Le Hir, G. & Ridgwell, A. 2020 The impact
964 of marine nutrient abundance on early eukaryotic ecosystems. *Geobiology* **18**, 139-151.
965 (doi:10.1111/gbi.12384).
- 966 [83] Kamennaya, N.A., Kennaway, G., Fuchs, B.M. & Zubkov, M.V. 2018 "Pomacytosis"—Semi-
967 extracellular phagocytosis of cyanobacteria by the smallest marine algae. *PLOS Biology* **16**,
968 e2003502. (doi:10.1371/journal.pbio.2003502).
- 969 [84] Laakso, T.A. & Schrag, D.P. 2018 Limitations on Limitation. *Global Biogeochemical Cycles* **32**,
970 486-496. (doi:10.1002/2017gb005832).
- 971 [85] Handoh, I.C. & Lenton, T.M. 2003 Periodic mid-Cretaceous Oceanic Anoxic Events linked by
972 oscillations of the phosphorus and oxygen biogeochemical cycles. *Global Biogeochemical Cycles* **17**,
973 1092. (doi:10.1029/2003GB002039).
- 974 [86] Alcott, L.J., Mills, B.J.W. & Poulton, S.W. 2019 Stepwise Earth oxygenation is an inherent
975 property of global biogeochemical cycling. *Science* **366**, 1333-1337. (doi:10.1126/science.aax6459).
- 976 [87] Tziperman, E., Halevy, I., Johnston, D.T., Knoll, A.H. & Schrag, D.P. 2011 Biologically induced
977 initiation of Neoproterozoic snowball-Earth events. *Proceedings of the National Academy of Sciences*
978 **108**, 15091-15096. (doi:10.1073/pnas.1016361108).
- 979 [88] Tarhan, L.G., Droser, M.L., Planavsky, N.J. & Johnston, D.T. 2015 Protracted development of
980 bioturbation through the early Palaeozoic Era. *Nature Geosci* **8**, 865-869. (doi:10.1038/ngeo2537).

- 981 [89] van de Velde, S., Mills, B.J.W., Meysman, F.J.R., Lenton, T.M. & Poulton, S.W. 2018 Early
982 Palaeozoic ocean anoxia and global warming driven by the evolution of shallow burrowing. *Nature*
983 *Communications* **9**, 2554. (doi:10.1038/s41467-018-04973-4).
- 984 [90] Dale, A.W., Boyle, R.A., Lenton, T.M., Ingall, E.D. & Wallmann, K. 2016 A model for microbial
985 phosphorus cycling in bioturbated marine sediments: Significance for phosphorus burial in the early
986 Paleozoic. *Geochimica et Cosmochimica Acta* **189**, 251-268. (doi:10.1016/j.gca.2016.05.046).
- 987 [91] Laakso, T.A. & Schrag, D.P. 2019 A small marine biosphere in the Proterozoic. *Geobiology* **17**,
988 161-171. (doi:10.1111/gbi.12323).
- 989 [92] Leys, S.P., Yahel, G., Reidenbach, M.A., Tunnicliffe, V., Shavit, U. & Reisswig, H.M. 2011 The
990 Sponge Pump: The Role of Current Induced Flow in the Design of the Sponge Body Plan. *PLOS ONE* **6**,
991 e27787. (doi:10.1371/journal.pone.0027787).
- 992 [93] Asadzadeh, S.S., Larsen, P.S., Riisgård, H.U. & Walther, J.H. 2019 Hydrodynamics of the leucon
993 sponge pump. *Journal of The Royal Society Interface* **16**, 20180630. (doi:doi:10.1098/rsif.2018.0630).
- 994 [94] Boyd, P.W. 2015 Toward quantifying the response of the oceans' biological pump to climate
995 change. *Frontiers in Marine Science* **2**. (doi:10.3389/fmars.2015.00077).
- 996 [95] Polimene, L., Saille, S., Clark, D., Mitra, A. & Allen, J.I. 2016 Biological or microbial carbon
997 pump? The role of phytoplankton stoichiometry in ocean carbon sequestration. *Journal of Plankton*
998 *Research* **39**, 180-186. (doi:10.1093/plankt/fbw091).
- 999 [96] Archibald, K.M., Siegel, D.A. & Doney, S.C. 2019 Modeling the Impact of Zooplankton Diel
1000 Vertical Migration on the Carbon Export Flux of the Biological Pump. *Global Biogeochemical Cycles*
1001 **33**, 181-199. (doi:10.1029/2018gb005983).

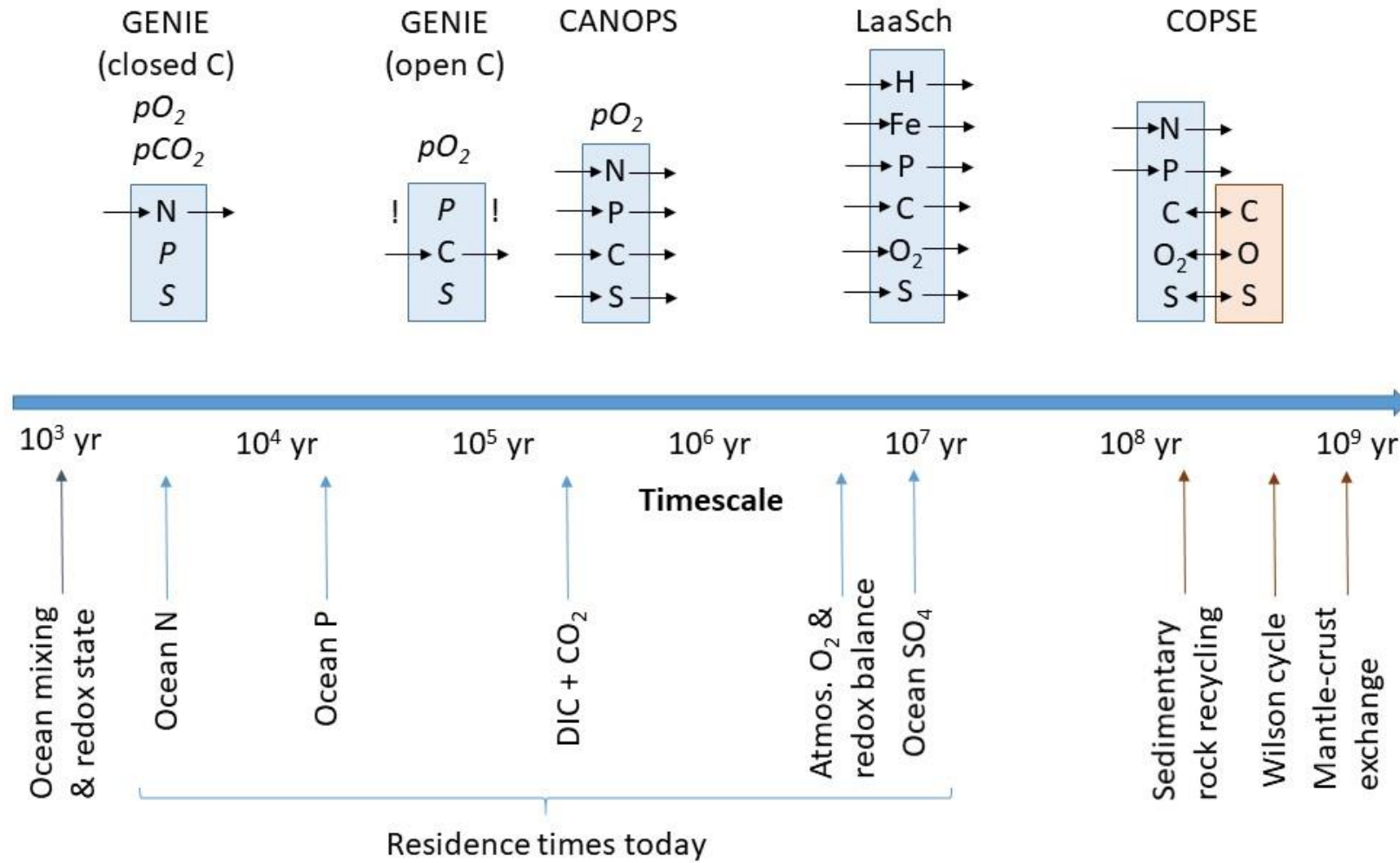
1002

1003

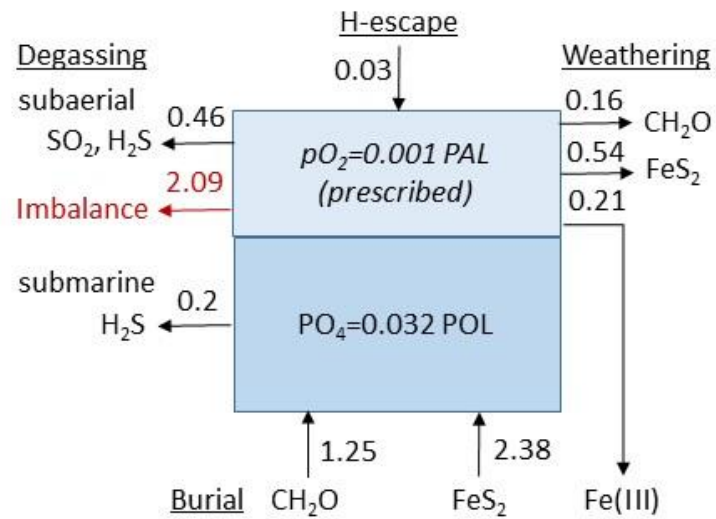
1004 Figure captions

1005 **Figure 1. Timescales of key Earth system processes and of model applicability.** Timescales of key
 1006 processes (below the line) include residence times of several key variable reservoirs today (DIC =
 1007 dissolved inorganic carbon), ‘redox state’ refers to deep ocean redox state, ‘redox balance’ refers to
 1008 Earth surface redox balance. Models are positioned above the line according to their approximate
 1009 (maximum) timescale of applicability, given their assumptions about which reservoirs are treated as
 1010 constant (in italics). Note that inferences about much longer timescales than indicated have been
 1011 made in some studies using CANOPS and LaaSCh (discussed in text). The major element cycles
 1012 captured within the ocean-atmosphere of each model are listed inside the blue box, ordered fast to
 1013 slow (from top to bottom) based on present day residence times. Incoming and outgoing arrows
 1014 indicate an open system representation for a cycle. Double headed arrows indicate exchange with
 1015 sedimentary rock elemental reservoirs, which are indicated in a brown box. Two ways of running
 1016 GENIE are indicated. Exclamation marks indicate a timescale inconsistency (where a fast variable is
 1017 treated as constant despite a slower variable being treated with an open system).

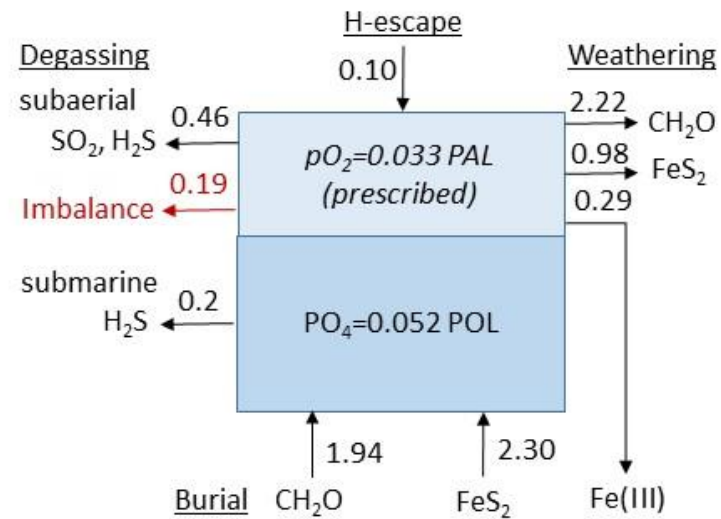
1018 **Figure 2. Earth surface redox (im)balance for proposed Proterozoic states of different models.**
 1019 Arrows indicate fluxes in Tmol O₂ (equivalents) yr⁻¹ (electrons flow in the opposite direction), PAL =
 1020 present atmospheric level, POL = present ocean level, CH₂O = organic carbon, FeS₂ = pyrite (but note
 1021 the stoichiometry may differ), “from” is used to indicate a source of electrons recognising the
 1022 gases/fluids will not be in that chemical form. **a)** CANOPS “Low O₂” scenario reproduced from Figure
 1023 5a of [71] with unmodelled reductant input ($\Phi_{\text{out}}[\text{Red}]$) indicated in red as redox “imbalance”. **b)**
 1024 CANOPS “High O₂” scenario reproduced from Figure 5b of [71]. **c)** LaaSCh “Low-O₂” scenario
 1025 reconstructed from [73] (note ‘pyrite’ burial flux actually has stoichiometry FeS). **d)** COPSE example
 1026 Proterozoic state from [47] assuming present day marine organic carbon burial flux, and indicative S
 1027 fluxes assuming sedimentary S reservoir is dominated by pyrite (in brackets because the S cycle can
 1028 then be excluded from the model and its redox balancing – see text).



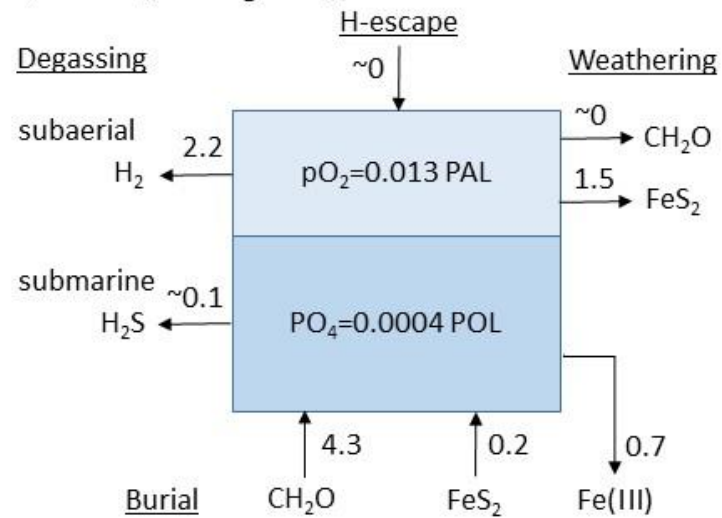
a) CANOPS ('low' O₂ case)



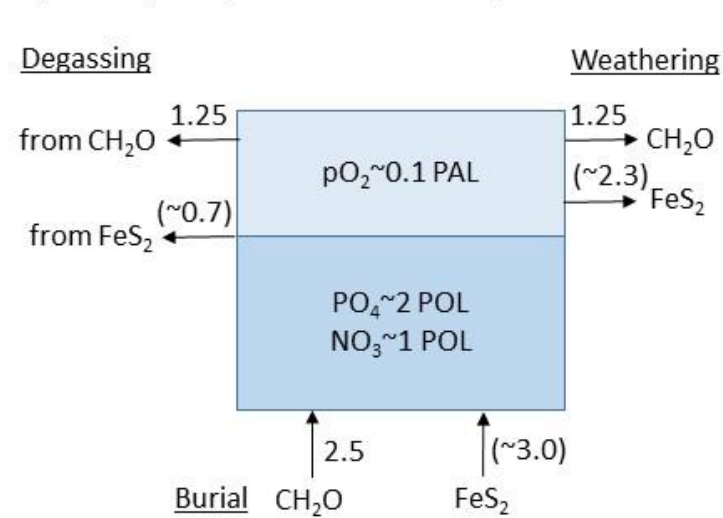
b) CANOPS ('high' O₂ case)



c) LaaSCh ('low' O₂ state)



d) COPSE (example Proterozoic state)



1031 Tables

1032 Table 1: Representation of key biogeochemical fluxes in three Proterozoic models

Cycle	Model		
	CANOPS	LaaSch	COPSE
Process			
Nitrogen			
Nitrogen fixation	compensates any N deficit	-	$\alpha (P-N/16)^2$
Denitrification (water)	$f([\text{NO}_3^-], [\text{O}_2])$	-	$f(\text{anoxia}, N)$
Denitrification (sediment)	$f([\text{NO}_3^-], [\text{O}_2], C_{\text{org}})$	-	$f(N)$
Phosphorus			
P weathering	Fixed flux: $0.18 \text{ TmolP yr}^{-1}$	Apatite (silicate) + oxidative	Silicate + carbonate + oxidative
P bioavailability to ocean	= P weathering	$0.33 \rightarrow 1$ as $p\text{O}_2$ $0.1 \rightarrow 1$ PAL (nominally Fe-mineral scavenging in estuaries)	= P weathering – P to land plants
P scavenging in ocean	α P upwelling * σ_{scav} parameter (0-1) (nominally by Fe-minerals)	α P (small flux)	-

Org-P burial	Complex function, $(C_{org}:P_{org})_{burial}$ increases with anoxia	P regeneration $\propto f(O_2, (\text{sedimentary oxic respiration} + SO_4 \text{ reduction} + Fe \text{ reduction}))$	$\propto C_{org}$ burial, $(C_{org}:P_{org})_{burial}$ increases with anoxia (250→4000)
Ca-P (authigenic) burial	Suppressed by anoxia		Suppressed by anoxia
Fe-P burial	Suppressed by anoxia		Suppressed by anoxia
Organic Carbon			
C_{org} degassing	-	(implicit in H_2 input)	$\propto C_{org}$ sedimentary reservoir
C_{org} oxidative weathering	$\propto pO_2^{0.5}$	$\propto pO_2$	$\propto pO_2^{0.5}$, C_{org} sedimentary reservoir
C_{org} burial land plants	-	-	50% of today's total C_{org} burial
Export/new production	P-limited (Michaelis-Menten), C:P increases 106→400 as P decreases	P-limited (linear), C:P=106	N-limited, C:P=106
Biological pump efficiency	Remineralisation= $f(O_2, NO_3, SO_4, CH_2O)$	Remineralisation= $f(O_2, SO_4)$	(Constant)
C_{org} burial efficiency	Enhanced by anoxia	Enhanced by anoxia	Optional $f(pO_2)$
Sulphur			(optional)
S degassing	0.7 TmolS yr^{-1} ($SO_2:H_2S=9:1$) subaerial + 0.1 TmolS yr^{-1} (H_2S) submarine	0.07 TmolS yr^{-1} (H_2S) submarine, (no subaerial)	Reduced \propto pyrite reservoir, Oxidised \propto gypsum reservoir

Pyrite weathering	Biotic \neq f(O ₂) + Abiotic=f(O ₂), complete oxidation pO ₂ >0.0035 PAL	0.8 TmolS yr ⁻¹ , complete oxidation pO ₂ >10 ⁻⁷ PAL	α pyrite sedimentary reservoir (complete oxidation)
Pyrite formation and burial	α sediment-water H ₂ S flux, burial efficiency suppressed by [O ₂]	Water-column and sediment formation	α C _{org} burial, [SO ₄], (pO ₂) ⁻¹
Gypsum weathering	Constant α assumed initial gypsum reservoir, assumed erosion rate	2.8 TmolS yr ⁻¹	α gypsum reservoir
Gypsum deposition	α [SO ₄]	α [SO ₄]	α [SO ₄]
Other O₂ terms			
H ₂ input	-	2.2 Tmol O ₂ eq yr ⁻¹	-
Hydrogen escape	α CH ₄	f(H), diffusion limited	-
Seafloor oxidation	-	α [O ₂] _d	-
Fe ²⁺ weathering	f(O ₂), buried on land	α silicate weathering, all goes to ocean	-
Fe ²⁺ hydrothermal	-	0.4 TmolFe yr ⁻¹	-
Fe ²⁺ ocean oxidation	-	α [O ₂][Fe ²⁺], some buried as siderite	-